ACCSCIENCE PUBLISHING

International Journal of Bioprinting

REVIEW ARTICLE

Comprehensive review on additive manufacturing of porous biomedical titanium alloys: Structural design, surface modification and applications

Shunyu Yao[1,2,3], Deyu Jiang[2,3], Vladimir Vasilievich Uglov[4], Fengcang Ma[1]*, Yanhua Chen[5]*, and Liqiang Wang[2,3]*

[1]School of Materials and Chemistry, University of Shanghai for Science and Technology, Shanghai, China

[2]State Key Laboratory of Metal Matrix Composites, School of Materials Science and Engineering, Shanghai Jiao Tong University, Shanghai, China

[3]National Facility for Translational Medicine, Shanghai Jiao Tong University, Shanghai, China

[4]Laboratory of NanoElectroMagnetics, Institute for Nuclear Problems, Belarusian State University, Minsk, Belarus

[5]School of Materials Science and Engineering, Xinjiang University, Xinjiang, China

***Corresponding authors:**
Fengcang Ma
(mafengcang@163.com)
Yanhua Chen
(cyh@xju.edu.cn)
Liqiang Wang
(wang_liqiang@sjtu.edu.cn)

(This article belongs to the *Special Issue: Intelligent bioprinting: From printable structures to functional systems*)

Citation: Yao S, Jiang D, Uglov VV, Ma F, Chen Y, Wang L. Comprehensive review on additive manufacturing of porous biomedical titanium alloys: Structural design, surface modification and applications. *Int J Bioprint*. 2026;12(3):026160143. doi: 10.36922/IJB026160143

Received: April 18, 2026

Revised: April 29, 2026

Accepted: May 4, 2026

Published online: May 4, 2026

Abstract

Titanium and its alloys have become the primary materials for orthopedic implants due to their excellent biocompatibility, mechanical properties, and corrosion resistance. However, traditional manufacturing techniques struggle to achieve complex porous structures, and their insufficient surface bioactivity limits their clinical performance. Additive manufacturing (AM) technology enables the precise fabrication of titanium implants with personalized shape, biomimetic porous structures, and gradient mechanical properties. The controllable porosity, pore size, and pore shape not only achieve mechanical compatibility with human bone tissue, but also provide an optimal microenvironment for cell adhesion, proliferation, and vascularization. During the process of designing porous structures, the auxiliary roles of finite element analysis (FEA) and machine learning (ML) play a crucial role in performance prediction and process optimization. To further enhance the bioactivity of AM titanium alloys, surface modification techniques such as mechanical, physical, chemical, and electrochemical methods have been widely employed. These modified coatings significantly improve the osseointegration efficiency, antibacterial properties, and corrosion resistance of implants without compromising the mechanical integrity of the substrate. Currently, AM titanium alloy implants have been successfully applied in joint replacements, dental prosthetics, and other fields. Through the synergistic effect of personalized design and surface functionalization, they demonstrate superior clinical application potential compared to traditional implants. This article systematically reviews the porous structure design, surface modification techniques, and application progress of AM titanium alloy implants, aiming to provide valuable insights for clinical applications.

Keywords: Additive manufacturing; Titanium alloy; Structural design; Surface modification

1. Introduction

The growing global demand for orthopedic implants requires materials with excellent biocompatibility, mechanical compatibility with bone tissue, rapid osseointegration, and long-term stability.[1-5] Titanium alloys are among the most widely used implant materials due to their favorable properties;[6-12] their primary applications are shown in Figure 1. However, traditional manufacturing limits complex porous structures, and their surfaces often exhibit insufficient bioactivity, leading to complications such as loosening and infection.[13,14] Additive manufacturing (AM) overcomes these limitations by enabling customized, biomimetic porous implants with gradient mechanical properties that enhance bone integration and cell growth.[15-19] Surface modification technology further compensates for these shortcomings by introducing bioactive layers, antibacterial elements, or tailored surface topologies to improve osseointegration, antibacterial performance, and long-term biocompatibility.[10,20-24]

In recent years, powder bed fusion (PBF) as the mainstream technologies of AM, have been widely applied to address issues in the field of medical implants.[25-27] PBF is a high-precision AM technology based on the principle of layer-by-layer powder spreading and selective melting by high-energy beams.[28] According to the type of heat source, it can be subdivided into laser powder bed fusion (LPBF) and electron beam powder bed fusion (EBPBF).[29,30] LPBF uses a fiber laser as the energy source, with a focused spot diameter of 20–50 μm, allowing precise control of heat input during the forming process. It offers core advantages such as high density, high forming accuracy, and excellent surface quality.[31] However, due to the rapid heating/cooling rates and significant rapid solidification characteristics in LPBF, AM titanium alloys tend to form ultra-fine acicular α' martensite and fine-grained structures, often leading to columnar grains that cause anisotropy.[32] Additionally, the high cooling rates result in high residual stresses, requiring subsequent heat treatment processes to improve mechanical properties.[28] EBPBF employs an electron beam with an acceleration voltage of 60–150 kV as the energy source and requires high-temperature preheating.[30] Due to the slow cooling rate of the molten pool, the overall temperature of the fabricated part remains high. AM titanium alloys generally form a balanced α+β structure, offering better plasticity and toughness with lower residual stress.[33] However, the surface roughness of the alloy is high and the dimensional accuracy is low, which makes it prone to powder adhesion and coarse-grained structure.

Mainstream AM processes such as LPBF and EBPBF enable the precise fabrication of porous titanium alloy bone implants with controllable pore structures. By adjusting pore size, porosity, and topological configuration, these implants achieve mechanical properties that match human cancellous bone, effectively alleviating stress shielding effects and providing three-dimensional interconnected channels for bone ingrowth.[16] In recent years, with the deep integration of computer technology and AM, finite element analysis (FEA) and machine learning (ML) have provided auxiliary support for the structural design of porous scaffolds.[34] FEA accurately simulates the stress distribution, deformation, and failure modes of porous titanium alloys under complex loads by performing calculations on discretized structural models of porous materials.[35] ML leverages high-throughput experimental data and FEA simulation data to establish mapping models between structural parameters and mechanical properties, thereby overcoming design efficiency bottlenecks.[36] However, the limited availability of high-quality sample data generated during the AM process makes ML models highly susceptible to overfitting, while insufficient model generalization remains a current challenge.

Although AM technology has become a core technical pathway for fabricating medical porous titanium alloy implants due to its unique advantages in the free design of complex geometries and personalized customization,[37] it is constrained by the inherent layer-by-layer melting and solidification mechanism of AM. Incomplete melting of powder particles and spheroidization-induced splashing result in a large amount of partially melted powder adhering to the strut surfaces, leading to significant surface roughness.[38] These surface defects not only considerably reduce the fatigue life of the components but may also cause loose particles on the implant surface to detach, triggering local inflammatory reactions and osteolysis. Additionally, titanium alloys are inherently bioinert materials, lacking the bioactivity required to actively induce bone regeneration on their surfaces. Relying solely on the passive bone conduction effect of the geometric structure makes it difficult to meet the clinical demands for early osseointegration.[39] Therefore, porous titanium alloy components fabricated by AM still face challenges related to insufficient surface quality and bioactivity. To address these bottlenecks, surface post-processing has become a critical step in enhancing the service performance

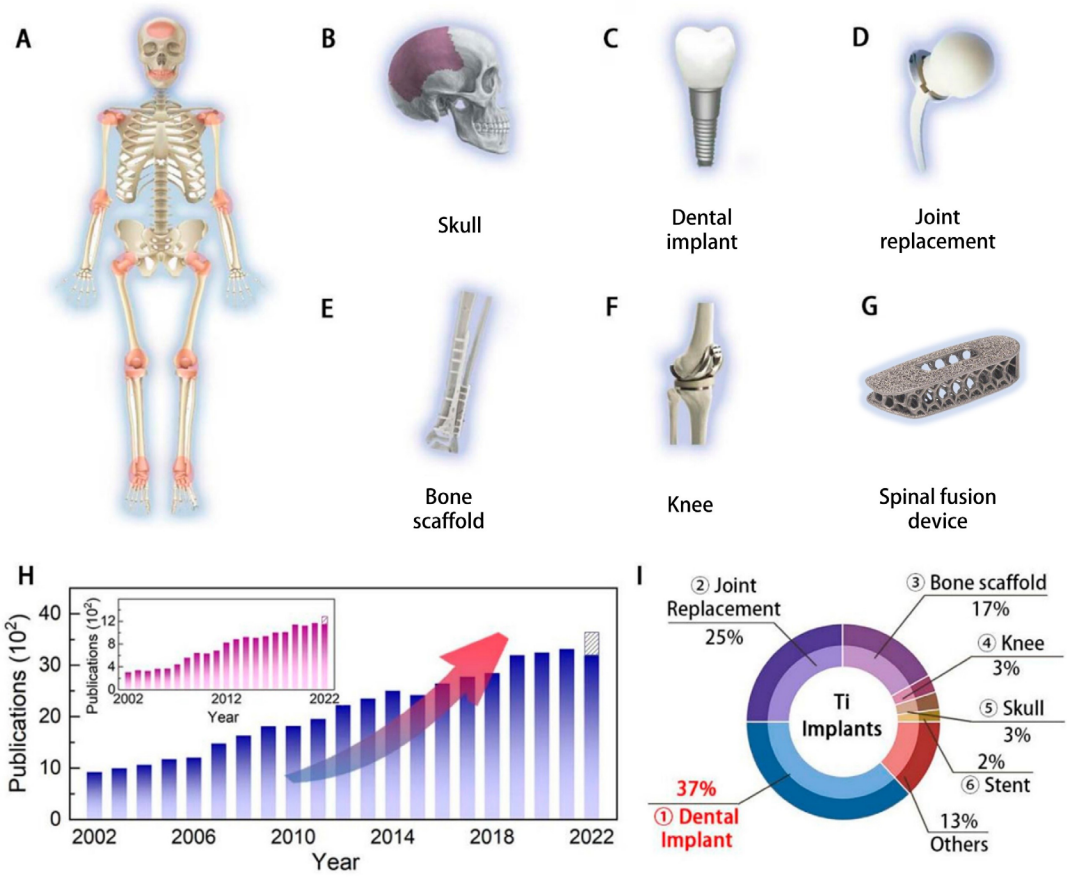

Figure 1. The application of Ti alloy bone implants and the scientific research publication trends in recent years. Reprinted with permission from Sun *et al.*[10] Copyright © 2023 American Chemical Society.

of AM-produced porous titanium alloys. The primary goals are to improve the material's biocompatibility, osseointegration efficiency, and antibacterial activity.[10,23,40] Current mainstream surface modification strategies include mechanical surface modifications (*e.g.*, sandblasting,[41] acid etching,[42] sandblasting-acid etching combined treatment[43]), physical surface modifications (*e.g.*, ion implantation,[44] magnetron sputtering[45]), chemical surface modifications (*e.g.*, alkali heat treatment,[46,47] hydrothermal synthesis,[20,48] sol-gel method[49]), and electrochemical surface modifications (*e.g.*, anodization,[50,51] micro-arc oxidation[52,53]), as illustrated in Figure 2. However, a single surface modification technique is often insufficient to meet the requirements for osteogenesis promotion, antibacterial properties, and corrosion resistance. Recent research has increasingly shifted toward the construction of composite coatings that synergistically combine multiple surface modification techniques. The aim is to integrate multidimensional functions—such as osteogenesis promotion, antibacterial activity, anti-inflammatory effects, and controlled drug release—on a single implant surface.[54] These primarily include smart responsive coatings based on pH, photothermal, and piezoelectric effects, as well as drug-delivery coatings.[55]

Recently, several reviews have addressed various aspects of AM titanium alloys for biomedical applications, yet most focus on isolated aspects of this multidisciplinary field. For instance, Blakey-Milner *et al.*[56] systematically evaluated the current use of metal AM across aerospace and medical fields, focusing on the role of process parameters in determining final part quality. Depboylu *et al.*[57] conducted a review on the design and fabrication of porous titanium alloy bone implants via AM, providing a detailed analysis of how pore structures affect biomechanical performance. Chen *et al.*[58] summarized the design principles and manufacturing methods of biomimetic porous scaffolds, discussing the impact of pore geometry on bone tissue regeneration. Regarding surface modification techniques for biomedical alloys, Vaiani *et al.*[59] systematically summarized surface modification

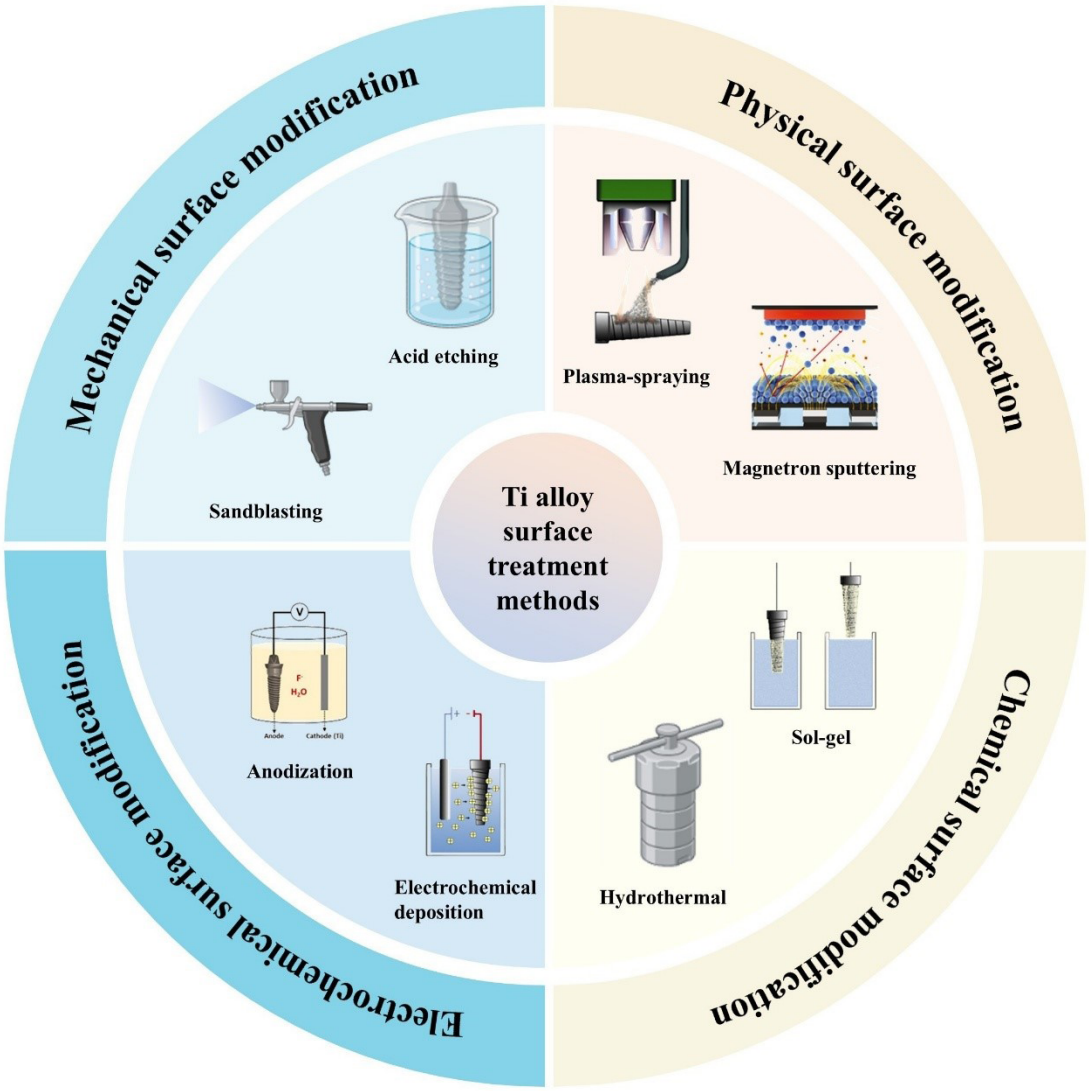

Figure 2. Different types of surface modification for titanium alloys. Reprinted with permission from Civantos *et al.*[40] Copyright © 2017 American Chemical Society. Reprinted with permission from Gulati *et al.*[51] Copyright © 2022 American Chemical Society.

strategies for titanium alloy implants, analysing the effects of various physical, chemical, and biological surface treatments on cellular responses. However, the aforementioned reviews focus on optimizing process parameters and controlling forming quality, yet they did not delve deeply into the topological design strategies of porous structures or the structure-property relationships between their mechanical and biological performance.[56] Some other reviews provide detailed analyses of pore structure design but pay insufficient attention to post-processing strategies for regulating inherent defects in AM.[57] Meanwhile, reviews concentrating on surface modification techniques often overlook the specific process context and geometric characteristics of AM porous structures, making it difficult to offer targeted guidance for practical clinical translation.[59] In fact, the comprehensive performance of AM-made porous titanium alloy implants depends on synergistic optimization across multiple stages. The manufacturing process determines the metallurgical quality and geometric accuracy of the matrix, structural design confers biomimetic mechanical properties and osteogenic functions to the implant, and post-processing surface modifications further regulate the surface physicochemical characteristics and bioactivity of the implant.

This paper aims to provide a comprehensive and systematic review of AM porous titanium alloys for medical applications, covering the following aspects: (i)

the design strategies for porous structures in orthopedic implants, including unit cell topology, porosity and pore size design, and biomimetic approaches for functionally graded structures; (ii) the auxiliary role of FEA and ML in the design of titanium alloy porous structures; (iii) the latest post-processing and surface modification techniques addressing surface issues of AM porous titanium alloys, covering conventional surface treatments and multifunctional coatings; and (iv) The clinical applications of AM porous titanium alloys in orthopedics, dentistry, and other fields. The overall framework is shown in Figure 3. By discussing the latest advances in the design optimization and clinical application of AM personalized porous titanium alloy orthopedic implants, this review offers forward-looking insights for the future development of bone implants.

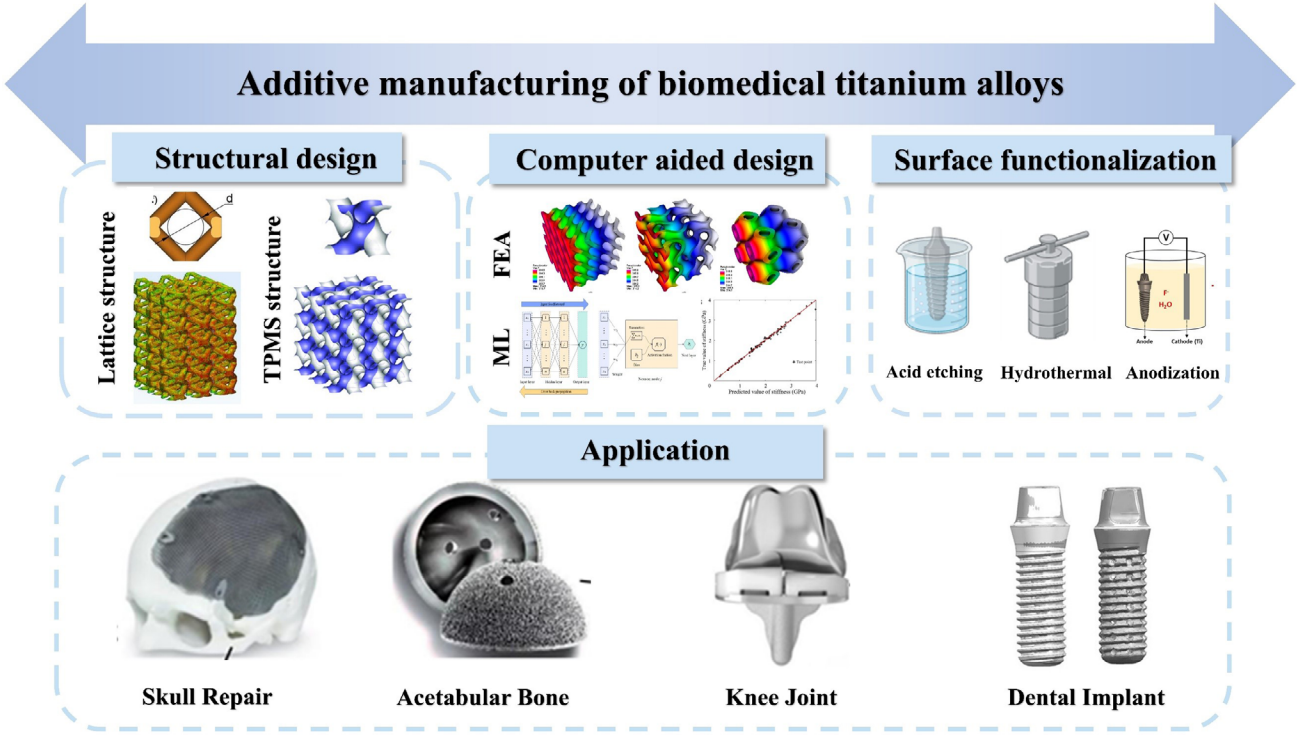

Figure 3. Framework diagram for the structure design, surface design and applications of titanium alloy porous bone implants. Reprinted with permission from Al-Ketan *et al.*[60] Copyright © 2019 Wiley. Reprinted with permission from Gawronska *et al.*[61] Copyright © 2021 MDPI. Reprinted with permission from Liu *et al.*[62] Copyright © 2023 Frontiers. Reprinted with permission from Sun & Shang.[63] Copyright © 2020 Scientific research. Reprinted with permission from Qin *et al.*[64] Copyright © 2023 Frontiers.

2. Design strategies for AM titanium alloy porous structures for orthopedic implants

2.1. Pore shape design

In AM of porous titanium alloys, pore shape serves as a critical structural parameter that not only determines the mechanical behavior of implants but also profoundly influences cellular response and bone ingrowth through local curvature, surface area, and fluid permeability.[17] Common pore shape types are primarily classified into lattice structures and triply periodic minimal surfaces (TPMS), as shown in Figure 4A. Lattice structures based on struts exhibit well-defined mechanical predictability but suffer from stress concentration.[65,66] In contrast, continuous smooth structures based on TPMS offer more uniform stress distribution, superior permeability, and are more conducive to nutrient transport and bone ingrowth. The appropriate selection of pore morphology is crucial for balancing the load-bearing capacity, fatigue life, and osteogenic functionality of implants.[67-69]

The lattice configuration, as a classic porous structure design for AM Ti alloy implants, demonstrates certain advantages in terms of manufacturability, surface roughness control, and printing precision, laying the foundation for its large-scale application in the biomedical field. Based on the periodic arrangement of discrete struts and nodes, lattice configurations such as BCC, FCC, and Rhombic Dodecahedron unit cells exhibit

strong parametric design flexibility. Key parameters like strut diameter and node spacing can be easily adjusted using CAD software to align with the forming principles of mainstream AM technologies like PBF. Ahmadi *et al.*[65] systematically compared the mechanical behaviour of six lattice unit structures and found that the rhombic dodecahedron structure, owing to its more uniform stress distribution, exhibited higher normalized stiffness and strength at the same relative density, whereas the cubic structure demonstrated lower mechanical efficiency due to stress concentration at the nodes. Arabnejad *et al.*[70] investigated the mechanical and osteogenic properties of porous Ti6Al4V tetrahedral lattices and octet-truss lattices. The octet-truss lattice exhibits superior mechanical performance at low porosity, but at high porosity, it is prone to a sharp decline in mechanical properties due to over-melting of struts and elliptical cross-section deformation. In terms of biological performance, the octet-truss lattice demonstrates a higher bone ingrowth rate, which is more conducive to early osseointegration. Lei *et al.*[71] fabricated four types of porous Ti6Al4V pedicle screws—Diamond, Orthogonal, Cubic, and Truss—using LPBF. FEA revealed that Orthogonal and Truss structures exhibit uneven stress distribution, are prone to deformation and failure, and have poor mechanical stability. In contrast, the Diamond structure shows the most uniform stress distribution and optimal mechanical stability, with its dual continuous channels free of dead zones, resulting in significantly superior permeability compared to other topologies. Parisien *et al.*[72] simulated the bone ingrowth stimulation effects of 24 lattice types based on a mechanoregulation model, distinguishing between bending-dominated and tension-dominated structures. In terms of biological performance, bending-dominated lattices such as BCC, diamond, FCC, G7, and octahedral structures exhibit higher tissue strain and fluid flow velocity, indicating significantly greater osseointegration potential compared to tension-dominated structures. Mechanically, bending-dominated lattices have lower modulus, better matching with bone tissue, and reduced stress shielding effects.

Although this lattice structure offers certain advantages in terms of manufacturability. In recent years, TPMS structures have garnered significant attention due to their smooth and continuous surfaces, highly interconnected pore networks, and morphology resembling natural trabecular bone.[73] The shape of the pores regulates the elastic modulus and compressive strength of the implant by altering the load-bearing modes of the struts (tension, bending, shear). Under the same porosity conditions, different unit structures exhibit distinct mechanical properties due to differences in load transfer paths and stress distribution patterns.[74] Furthermore, the geometry of the pores influences cell behavior through local surface curvature and specific surface area, while also affecting the transport of nutrients, angiogenesis, and bone ingrowth through connectivity and permeability.[75] Research indicates that cells are sensitive to substrate curvature, where moderately concave surfaces can promote cell spreading and adhesion, whereas sharp convex corners may inhibit cell migration. The continuously curved surfaces of TPMS structures, with their highly interconnected pore networks and high permeability, provide a more favorable geometric environment for cell adhesion and migration.[76,77] Bobbert *et al.*[78] fabricated four types of TPMS porous Ti6Al4V structures: Primitive, I-WP, Gyroid, and Diamond. In terms of stiffness, yield strength, and fatigue life, the order was D≈I-WP>G>P. Regarding permeability, the order was P>D≈G>I-WP. Primitive, with the highest permeability and lowest modulus, is suitable for non-load-bearing bone defect filling. I-WP, with its high specific surface area and excellent fatigue performance, is suitable for medium-load-bearing implants such as interbody fusion cages. Gyroid offers a balance between mechanical and permeability properties, making it suitable for periarticular repair scaffolds. Diamond, with optimal stiffness, strength, and fatigue resistance, is suitable for high-load-bearing sites such as the femur. Deng *et al.*[79] systematically compared four types of topological Ti6Al4V porous scaffolds fabricated by LPBF. In terms of permeability, the D structure exhibited the smallest internal flow velocity difference, the longest and most uniformly distributed streamlines, allowing fluid to fully penetrate the scaffold, balancing nutrient transport and cell adhesion, and achieving the highest permeability efficiency. Simultaneously, the D structure also demonstrated the best compressive strength and bone ingrowth, making it the preferred topological configuration for high-load-bearing bone defect repair. Gandhi *et al.*[80] systematically reviewed the mechanical, fatigue, and osseointegration properties of four categories of AM topological structures: strut-based lattices, TPMS, random porous structures, and gradient structures. TPMS structures, with their continuous and smooth surfaces, achieve the best balance among mechanical properties, permeability, and bone ingrowth performance. Mechanically, Gyroid and Diamond, at 60–70% porosity, exhibit elastic moduli (0.5–3 GPa) highly compatible with cancellous bone, while their continuous surfaces without sharp nodes significantly eliminate stress concentration, resulting in excellent fatigue performance. In terms of permeability, the dual-continuous interconnected channels of TPMS structures have no flow dead zones, with permeability reaching 10^{-9}–10^{-10} m^2.

The pore shape is a key design variable that determines the overall performance of 3D-printed porous titanium

alloy implants. In summary, lattice structures remain widely used due to the convenience of parametric design, but stress concentration at nodes and relatively low biological response limit their performance in high-demand applications. The TPMS structure achieves the optimal balance among strength, fatigue resistance, permeability and osteogenic properties, better meeting the biomimetic and service requirements of bone implants.

2.2. Pore size and porosity design

The pore size and porosity of AM porous titanium alloy implants are regarded as two core structural parameters. These parameters not only directly influence the mechanical properties but also impart essential biological functions to the implants.[81] An appropriate pore structure enables the elastic modulus to approach that of human bone, facilitates the growth, migration, and proliferation of osteoblasts, and allows the transport of nutrients and oxygen within the structure.[82,83] The effects of pore size and porosity on the performance of porous titanium alloy implants are not independent; therefore, these two factors are discussed together.

In terms of mechanical properties, pore size and porosity significantly affect key indicators by altering the effective load-bearing area and structural support mode of the implant. For porous titanium alloys prepared by LPBF, Taniguchi *et al.*[83] fabricated porous titanium implants with pore sizes of 300, 600, and 900 μm using LPBF technology and implanted them into rabbit tibiae for *in vivo* experiments. At 4 weeks post-implantation, the group with a pore size of 300 μm exhibited the highest bone ingrowth rate. However, after 8 weeks, the group with a pore size of 600 μm showed more mature bone tissue and deeper bone ingrowth depth. This indicates that smaller pore sizes are beneficial for the early proliferation and differentiation of osteoblasts. Liang *et al.*[84] employed Voronoi-Tessellation mathematical modeling combined with LPBF technology, demonstrating that 65–75% porosity with highly irregular porous structures can achieve a balance of low modulus, balanced strength, and excellent osteogenic activity. Chen *et al.*[85] used LPBF technology to prepare isotropic octahedral lattice Ti6Al4V ELI porous scaffolds, with full factorial variable combinations of designed pore sizes of 500/600/700 μm and porosities of 60%/70%. The results showed that the combination of a pore size of 500 μm and a porosity of 60% exhibited the optimal osteogenic performance, with strength sufficient to meet the requirements of load-bearing sites such as the femur and tibia. Yan *et al.*[86] further demonstrated that due to the high curvature-driven effect, cells could spread uniformly along the struts and penetrate into the internal pores of scaffolds with a pore size of 500 μm, resulting in optimal osteogenic activity. Zhang *et al.*[87] fabricated cubic lattice pure titanium scaffolds using LPBF, with designed pore sizes of 400/700/900 μm and porosities of 40%/70%/90%. Mechanical results indicated that porosity was the absolute dominant factor, while pore size had almost no effect on mechanical properties. Regarding osteogenic performance, at 70% porosity, the 700 μm pore size exhibited optimal osteogenic gene expression, alkaline phosphatase (ALP) activity, calcium nodule deposition, and *in vivo* bone ingrowth. A pore size of 400 μm was too small to allow sufficient material exchange, while a pore size of 900 μm was too large for cells to be effectively retained. Ouyang *et al.*[88] used computational fluid dynamics (CFD) analysis to find that as the pore size increased from 400 μm to 650 μm, the permeability and fluid flow velocity of the scaffold increased linearly, while the wall shear stress reached a peak, promoting osteoblast penetration, adhesion, and differentiation. Beyond 650 μm, the shear stress decreased, leading to reduced cell proliferation and bone ingrowth efficiency. Ultimately, the bone volume fraction in the 650 μm group was significantly higher than that in other pore size groups, as shown in Figure 4B. Kelly *et al.*[89] showed that increasing porosity from 50% to 70% significantly enhanced ALP activity and mineralized matrix deposition in osteoblasts. This finding was also confirmed *in vivo*. As observed by Pobloth *et al.*[90] in a sheep critical-sized bone defect model, titanium mesh scaffolds with high porosity (approximately 70%) outperformed low-porosity groups in terms of bone bridging speed and new bone volume fraction. However, excessively high porosity may reduce mechanical stability, leading to implant micromotion and subsequently inhibiting osseointegration.[91]

Due to the differences in forming accuracy between EBPBF technology and LPBF, their suitable pore sizes and porosity levels also vary. Goto *et al.*[92] used EBPBF technology to fabricate lattice-type large-pore interconnected porous Ti6Al4V implants with a pore size range of 880–1400 μm and an average porosity of 57.5%. The large-pore design ensured thorough powder removal within the pores, no internal blockages, and 100% structural connectivity, providing a foundation for subsequent fluid permeability and bone ingrowth. Zhang *et al.*[93] employed EBPBF to prepare trabecular bone-mimetic Ti6Al4V porous scaffolds. A porosity of 65%–75% and a pore size of 700–1,000 μm achieved an optimal balance among mechanical strength, elastic modulus, and osteogenic performance, making them suitable for bone repair implants in non-load-bearing and light-load-bearing areas. Hara *et al.*[94] utilized EBPBF technology to fabricate diamond-structure implants with pore sizes of 500, 640, 800, and 1000 μm, with an average porosity of 70%. The groups with pore sizes of 500–800 μm showed

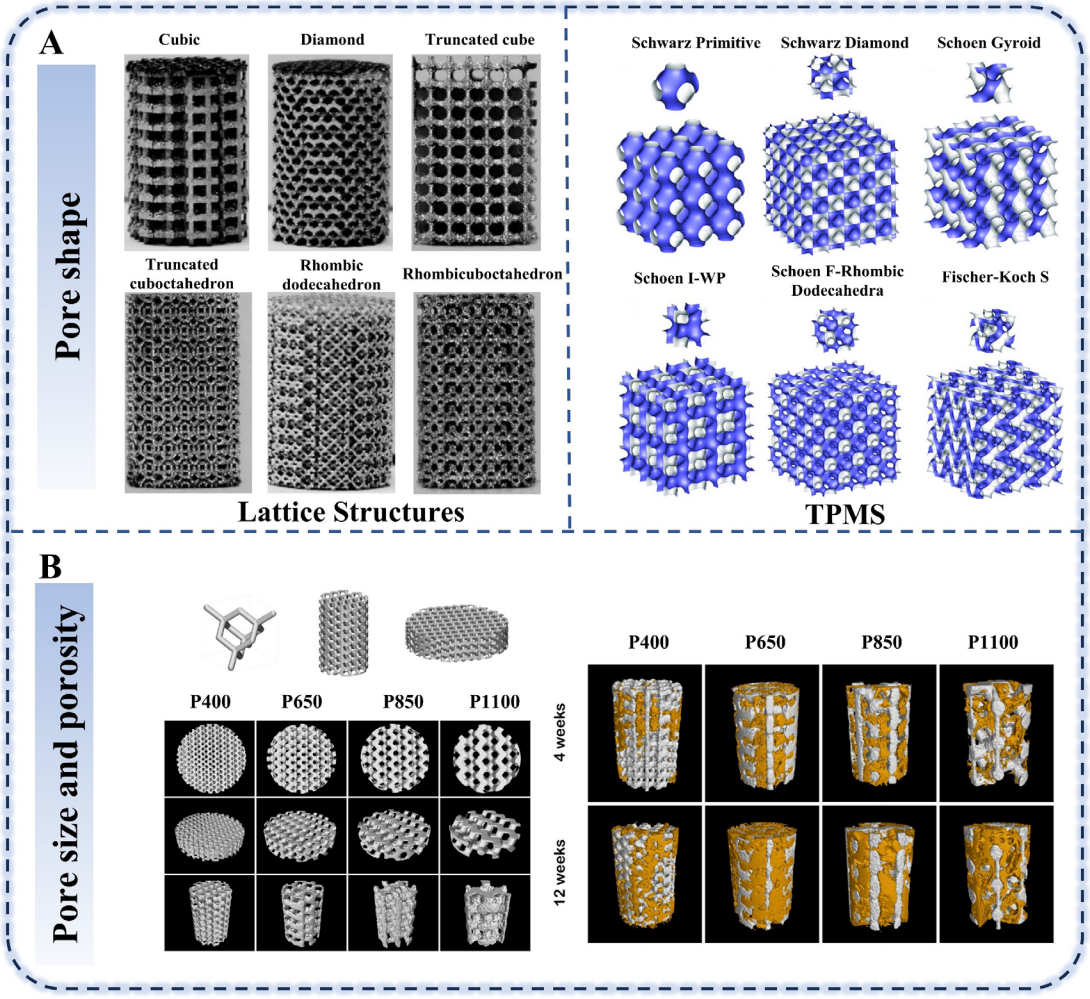

Figure 4. The design of pore shape, pore size and porosity of the AM porous structure. (A) AM of porous Ti alloys with lattice structure and TPMS structure. Reprinted with permission from Ahmadi *et al.*[65] Copyright © 2015 MDPI. Reprinted with permission from Al-Ketan *et al.*[60] Copyright © 2019 Wiley. (B) Porous titanium alloys with different pore size. Reprinted with permission from Ouyang *et al.*[88] Copyright © 2019 Elsevier.

a continuous increase in bone integration strength over time, with the 640 μm group reaching a bonding strength of 704.6 N at 12 weeks. This study provided a basis for the fabrication of EBPBF porous acetabular cups and joint prostheses. Wang *et al.*[95] used EBPBF to prepare irregular porous Ti6Al4V scaffolds mimicking trabecular bone. With a fixed high porosity, three pore size groups—800, 900, and 1,000 μm—were established to analyze the effects of pore size on elastic modulus, wettability, cell adhesion and proliferation, and osteogenic gene expression. The aim was to establish the relationship between pore size and performance in irregular bionic structures. The 1,000 μm group exhibited an elastic modulus closest to that of cancellous bone, providing the best anti-stress shielding effect. *In vitro* cell experiments showed that cell adhesion, proliferation, ALP activity, and osteogenic gene expression significantly increased with larger pore sizes. The mechanism lies in the enhanced permeability provided by larger pores, which improves nutrient and oxygen transport while strengthening mechanical signal transduction in cells, thereby promoting osteogenic differentiation.

In summary, pore size and porosity play a crucial regulatory role in bone tissue ingrowth and angiogenesis. Smaller pores, while enhancing structural stiffness and mechanical strength, can hinder cell migration and tissue infiltration, thereby affecting the biological functionality of the scaffold. In contrast, larger pores are more conducive to cell migration and vascular ingrowth, significantly improving osseointegration and vascularization, but at the cost of reduced structural and mechanical stability. Therefore, personalized design of pore size tailored to specific load-bearing scenarios is particularly critical.

Appropriate porosity and pore size can achieve a balance between osteogenic performance and compressive strength. Table 1 summarizes the characteristics of typical AM porous titanium alloy scaffolds. For bone defect repair, bone implants fabricated via LPBF have a suitable porosity range (60–70%), enabling effective elastic modulus matching with the host bone while ensuring sufficient load-bearing capacity. The appropriate pore size range is 500–700 μm, which balances early cell attachment with later-stage vascularization and bone ingrowth capabilities. Bone implants prepared by EBPBF have a suitable porosity range of 70–75% and a pore size of 800–1,000 μm.

Table 1. Summary of porous titanium alloys with different pore size and porosity.

Materials	AM processes	Pore size (μm)	Porosity (%)	Elastic modulus (mPa)	Compressive strength (mPa)	Key biological performance	Clinical application	Ref.
Pure Ti	LPBF	300, 600, 900	65	557.4–661.4	36.2–51.4	The 600 μm group has the fastest bone ingrowth rate and the best fixation performance.	Spinal fusion device	[83]
Ti6Al4V	LPBF	400–1,000	48.83–74.28	1,930–5,240	44.9–237.5	The cell proliferation and osteogenic differentiation are optimal at a porosity of 65% to 75% for the scaffold.	Joint replacement prosthesis (load-bearing bone)	[84]
Ti6Al4V	LPBF	500, 600, 700	60, 70	2,100–4,700	71–190	500 μm, 60% optimal for scaffold bone ingrowth	Repair of load-bearing bone defects, such as femur and tibia	[85]
Ti6Al4V	LPBF	500, 600, 700	60, 70	2,100–4,700	73–207	60% porosity offers better mechanical compatibility with human bones	Repair of load-bearing bone defects, such as femur and tibia	[86]
Pure Ti	LPBF	400, 700, 900	66.1, 72.3, 80.7	1,000–12,900	10.9–184.8	700 μm, 70% results in the optimal osteogenesis. The pore size has a greater influence than the porosity.	Repair of bone defects such as femoral condyle defects	[87]
Pure Ti	LPBF	400, 650, 850, 1,100	68	-	40-60	650 μm aperture for fluid mechanics compatibility, optimal bone ingrowth	Repair of non-load-bearing bone defects	[88]
Ti6Al4V	EBPBF	315, 485, 574	33.8, 50.9, 61.3	1,700–3,700	33.1–115.2	Cells with a pore size of 300–400 μm exhibit the best adhesion to osteogenic substances.	Repair of non-load-bearing bone defects	[91]
Ti6Al4V	EBPBF	880–1,400	57.5	3570	78.9	Better connectivity with larger aperture	Repair of extensive bone defects	[92]
Ti6Al4V	EBPBF	766–1,319	61.44–79.67	390–618	30.27–80.34	-	Non-load-bearing and light load-bearing area bone repair implants	[93]
Ti6Al4V	EBPBF	500, 640, 800, 1,000	65–70	1,200–1,600	-	800 μm bone grows in the optimal manner	Porous acetabular cups and joint prostheses	[94]
Ti6Al4V	EBPBF	800, 900, 1,000	-	10,430–19,170	115.43–333.35	The larger the aperture, the lower the modulus. At 1000 μm, osteogenic differentiation is the best.	Repair of extensive bone defects	[95]

Abbreviations: EBPBF: Electron beam powder bed fusion; LPBF: Laser powder bed fusion.

2.3. Biomimetic design of functionally gradient porous structures

Although uniform porous structures have proven to be effective for biomedical implant materials, they struggle to meet the demands of complex bone grafting. In recent years, gradient porous structures have shown significant potential. Natural bone tissue exhibits a distinct hierarchical gradient structure, composed of an outer layer of dense cortical bone and an inner layer of cancellous bone. The difference in porosity between cortical and cancellous bone leads to a notable disparity in their mechanical properties, with elastic moduli ranging from 3–20 GPa for cortical bone and 0.1–4.5 GPa for cancellous bone. Therefore, gradient porous structures can achieve excellent mechanical compatibility with natural bone. Specifically, an outer layer with lower porosity can provide initial mechanical support, while an inner layer with higher porosity promotes bone ingrowth and long-term integration.[96] Yao *et al.*[97] used parametric modeling to fabricate three sets of scaffolds based on Gyroid TPMS units, with porosity varying continuously along the radial direction. These scaffolds—dense on the outside and porous on the inside—perfectly mimic the structural characteristics of natural bone. Compared to uniform structures, radial gradient scaffolds enable more uniform stress transmission from the edge to the center, significantly reducing stress concentration. Additionally, this structure offers a larger specific surface area, providing more sites for cell adhesion and proliferation. The results show that a radial gradient structure with 70% internal porosity achieves an elastic modulus of 5.2 GPa and a yield strength of 296.02 mPa, making it most suitable for bone repair in load-bearing areas such as the femur and acetabulum. Arabnejad *et al.*[96] used LPBF technology to fabricate a fully porous titanium alloy femoral stem. Their study employed a tetrahedral lattice unit design and multi-scale asymptotic homogenization theory to optimize the spatial gradient relative density distribution of the femoral stem. This optimization achieved a continuous stiffness transition from proximal to distal and from surface to core, enabling precise matching of the prosthesis modulus with the mechanical properties of the host femur. Among these, a gradient fully porous prosthesis with 70% internal porosity and a pore size of 500 μm reduced bone resorption due to stress shielding by 75%.

In addition to gradient porous structures, inspired by natural materials such as nacre, tortoise shells, and sea urchin spines, biomimetic structural design has garnered widespread attention in the field of high-performance bone tissue scaffolds and biomaterials.[98] The sea urchin spine is a plant-like hierarchical lightweight structure with a porous internal skeleton composed of pores of varying sizes and distributions. These pores exhibit a gradual gradient from the base to the tip of the spine, with larger pore sizes and lower solid density at the base, and smaller pore sizes and higher solid density at the tip, forming a bicontinuous gradient porous structure. Inspired by the multilevel gradient structure of natural sea urchin spines, Zhang *et al.*[99] used LPBF technology to fabricate a gradient porosity and tapered topology pentamode metamaterial biomimetic porous titanium alloy scaffold. Compared to uniform lattice structures, the gradient pentamode scaffold exhibited an elastic modulus of 0.4–1.2 GPa, which closely matches that of cancellous bone. Its energy absorption efficiency increased by 77.75%, and the yield strength remained stable at 15–40 mPa, meeting the requirements for load-bearing support. Additionally, the gradient structure increased permeability by 27.27%, resulting in a more uniform fluid flow velocity distribution, with no flow dead zones or turbulence, and a significant increase in streamline length. Jia *et al.*[98] designed a biomimetic irregular aperiodic gradient porous material using a generative computational framework, simulating the disordered gradient microstructure of natural bone to achieve precise control over stress distribution, as shown in Figure 5. The irregular gradient scaffold reduced interfacial stress concentration by over 60% and significantly improved resistance to loosening and fatigue. Furthermore, the scaffold's channels mimic the topology and curvature of natural bone trabeculae, promoting cell adhesion, spreading, and migration that more closely resemble physiological conditions, with a 40% increase in deep bone ingrowth. Ye *et al.*[100] designed primary and secondary fractal gradient porous Ti-Cu alloy scaffolds based on the G-type TPMS structure. The secondary fractal gradient scaffold exhibited an elastic modulus of 1.654–3.636 GPa and a compressive yield strength of 50.9–111.5 mPa, significantly lower than that of primary structures with the same porosity, allowing for more precise matching with the modulus of cancellous bone and reducing the risk of stress shielding. Zhang *et al.*[101] proposed a design method for biomimetic gradient G-type TPMS scaffolds with quantitatively adjustable pore sizes. The scaffold's compressive failure mode is a safer layer-by-layer extrusion densification, with energy absorption efficiency increasing by 9.6%–19.5% compared to uniform structures. The scaffold with optimal parameters (gradient pore size 0.35–1.00 mm, average porosity 63%) is suitable for clinical applications such as metaphyseal and periarticular regions, where gradient mechanical properties and efficient bone ingrowth are required.

Gradient porous structures enable continuous variation in porosity and pore size from the surface to the core, as well as from the proximal to the distal end, significantly

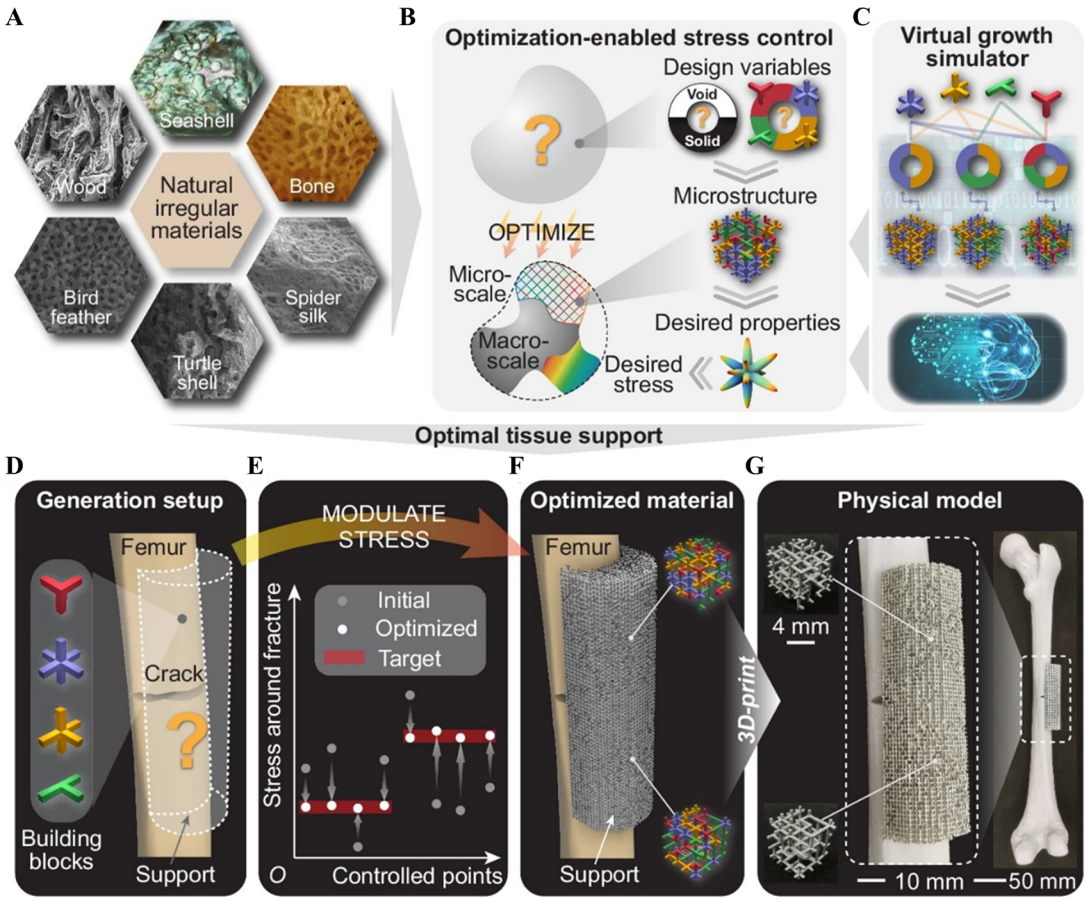

Figure 5. Natural irregular bionic porous structure design. (A–C) Design of porous materials at macroscopic and microscopic scales based on natural irregular materials, (D–G) generation and fabrication of irregularly structured materials for pelvic fracture repair. Reprinted with permission from Jia *et al.*[98] Copyright © 2024 Nature.

optimizing stress distribution. The bone-inspired gradient design, characterized by a dense outer layer and a sparse inner region, enhances interface stability and overall strength. The high-porosity internal zone reduces the modulus to alleviate stress shielding, resulting in smoother stress transfer, reduced stress concentration, and adequate space for bone ingrowth. Furthermore, natural bone tissue is not a uniform periodic porous structure but exhibits irregular, non-periodic, and hierarchical characteristics at multiple scales. Recently, inspired by natural materials, irregular non-periodic gradient biomimetic structures—by simulating the biological architecture of bone—have demonstrated significant potential in mechanical matching, stress distribution optimization, permeability and mass transfer, and cellular biological responses.

2.4. Numerical simulation assisting in AM structure design

Numerical simulation is a key auxiliary tool for revealing the intrinsic mechanisms of the additive manufacturing process and promoting the development of this technology toward high precision and industrialization. As a core numerical simulation method, FEA plays an irreplaceable role in the regulation of pore characteristics, optimization of mechanical properties, evolution of thermal stress, and adaptation of biological functions in AM porous titanium alloys.[102-104] By calculating the representative volume element of porous materials, FEA can intuitively simulate the force transmission and stress distribution patterns inside porous scaffolds, providing good predictive and simulation capabilities for subsequent experiments.[105]

In the evaluation of the mechanical properties of titanium alloy porous scaffolds, FEA has been proven to be an efficient and reliable simulation method. FEA can intuitively display the magnitude and distribution of stress at key locations such as the pore walls and unit nodes of the porous scaffolds.[106] Zhang *et al.*[103] optimized the

hexagonal porous structure of TC4 alloy via FEA. When the wall thickness exceeded 200 μm, the alloy achieved a yield strength of 550 mPa and an elastic modulus of 14.4–15.4 GPa, exhibiting both excellent mechanical properties and biocompatibility. Yu *et al.*[107] compared the mechanical properties and permeability of three topological structures (Primitive, Gyroid, BCC) of Ti_6Al_4V porous scaffolds, as shown in Figure 6A. The Gyroid structure exhibited the highest compressive strength (392.1 mPa) and tensile strength (321.3 mPa) due to its larger cross-sectional area, while the BCC structure, with its simpler topology and larger pore size, demonstrated optimal permeability. These findings provide a basis for selecting porous scaffold architectures. In addition, for the design and optimization of gradient porous complex structures, FEA can quickly predict the mechanical properties of scaffolds, precisely optimize the stiffness distribution and strain range of porous implants, and significantly shorten the development cycle. Shum *et al.*[108] addressed the issues of uneven stress distribution, excessively high or low local strain, and significant differences in bone ingrowth in traditional homogeneous porous implants under eccentric loading conditions in the knee joint. They established a FEA model of a sheep knee joint to simulate the von Mises stress and octahedral shear strain distributions in homogeneous and gradient porous titanium implants with different stiffnesses. Through gradient stiffness optimization, the FEA confirmed that the gradient Ti3 (with a surface stiffness of 0.3 GPa and a core stiffness of 0.1 GPa) could redistribute stress and strain, stabilizing the overall strain within the efficient osteogenic range of 1–3.75%. Moussa *et al.*[109] employed multiscale homogenization theory combined with density topology optimization and FEA to design a gradient porosity fully porous titanium alloy acetabular reinforcement cage. Compared to solid prostheses, the gradient porous structure reduced peak contact stress by 21.4%, peak interface micromotion by 26%, and stress concentration areas. The peak von Mises stress was reduced by 43%, fundamentally alleviating stress shielding.

In the field of personalized design and optimization of biomedical implants, FEA facilitates the achievement of mechanical compatibility and functional adaptation between implant structures and human tissues. Srivastava *et al.*[110] integrated nTopology software with CT-scanned anatomical data to design personalized Ti_6Al_4V hip prosthesis stems featuring four lattice structures: Voronoi, Gyroid, Schwarz, and Hexagonal, as shown in Figure 6B. ANSYS static loading FEA revealed that the Hexagonal lattice structure performed optimally, exhibiting a von Mises stress of only 553 mPa and a total deformation of 0.565 mm. Compared to the Voronoi structure, stress was reduced by 78%, and deformation decreased by 4.6%, effectively mitigating stress shielding and promoting osseointegration. Naqvi *et al.*[102] designed a Gyroid-structured dental implant with axial gradient porosity (40–80%). FEM demonstrated that the von Mises stress–strain values around the cortical bone (stress: 60 mPa, strain: 100–3,000 με) were within the favorable range for bone ingrowth. Cell experiments further confirmed that regions with 60% porosity exhibited optimal cell proliferation and differentiation. Peng *et al.*[111] constructed a non-uniform mandibular finite element model based on computed tomography (CT) scans of patient, integrating FEA with topology optimization and Mechanostat theory to design a biomimetic, hierarchical porous titanium alloy mandibular implant. This implant enables stress to be uniformly transmitted along physiological trajectories and eliminates stress concentration.

FEA can accurately predict stress concentration, quantitatively evaluate stress shielding and interface micromotion, and rapidly iterate parameters such as aperture, porosity, and gradient structures. It provides a precise and efficient numerical tool for optimizing the process parameters of porous materials and enhancing implant performance. However, FEA still faces some issues. For example, simulations of porous structures often rely on homogenization and equivalent model simplifications, making it difficult to fully capture irregular pillar deformations and mechanical anisotropy, which leads to idealized stress calculations. Additionally, FEA is more focused on computing mechanical indicators such as stress, strain, and displacement, and cannot directly simulate cell behavior and bone ingrowth. Predictions of osteogenesis rely on indirect derivations.

2.5. Machine learning assists in the design of porous titanium alloys

The rapid development of AM technology has significantly increased the design freedom of porous titanium alloy implants, but it has also brought challenges such as an explosion in parameter space and high computational costs to traditional trial-and-error experimental design. As an intelligent data-driven tool, ML offers substantial advantages in multi-parameter complex structural design due to its powerful nonlinear mapping and multi-objective optimization capabilities.[112] Currently, ML-related research primarily focuses on forward prediction and inverse design. Forward prediction is used to establish a mapping relationship between structural parameters and mechanical properties, enabling rapid performance prediction and evaluation. Inverse optimization takes target performance as input and inversely deduces the optimal structural parameter configuration, thereby achieving efficient performance-driven design.[113-115]

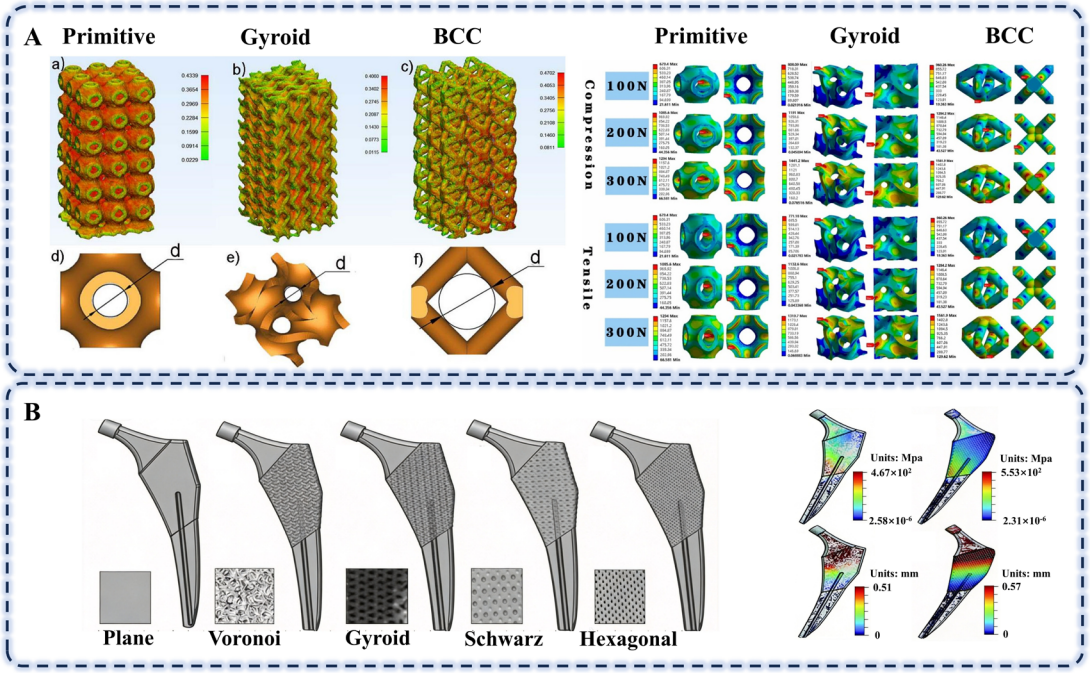

Figure 6. Simulation of the mechanical performance of additively manufactured titanium alloys based on finite element analysis. (A) Different types of support designs and mechanical performance simulations are conducted through finite element analysis: primitive scaffolds; gyroid scaffolds; BCC scaffolds. Reprinted with permission from Yu *et al.*[107] Copyright © 2020 Elsevier. (B) Femoral model with five lattice structures and von Mises stress simulation by finite element analysis. Reprinted with permission from Srivastava *et al.*[110] Copyright © 2025 Taylor & Francis.

Metamaterial design relies on expert experience and consumes significant effort. One of the core advantages of ML forward prediction is its ability to significantly reduce dependence on scientists' prior knowledge. Using models such as backpropagation neural networks (BPNN), a mapping relationship between structural parameters and mechanical properties can be established. Once the model is sufficiently trained and validated, it can serve as an efficient surrogate model, generating outputs in real-time from new inputs, thereby replacing extensive preliminary FEA calculations.[116] Peng *et al.*[117] proposed an intelligent design framework called GADMALL. Taking G-type TPMS porous structures as the subject, they generated a vast number of candidate structures using a 3D convolutional autoencoder, and then predicted elastic modulus and yield strength with a 3DCNN. The heterogeneous porous scaffold designed via ML exhibits a yield strength increase of over 30% compared to the uniform structure, with its elastic modulus precisely matching the range of cancellous bone to cortical bone (2.5–5 GPa), as shown in Figure 7. Hu *et al.*[118] combined Bayesian optimization with FEA to achieve rapid optimization with small sample data. The optimal parameter combination was wall thickness (Pt = 0.28 mm), constant (Pc = −0.49), and number of cells (Pa = 3.5), achieving a strength of 1.21 GPa and permeability of (4.03×10^{-9} m^2), simultaneously meeting the mechanical and mass transfer requirements for bone implantation. ML reveals that the wall thickness and the number of units determine the strength, while the constant Pc regulates the permeability.

In addition to forward prediction, ML also enables inverse design by taking key clinical indicators such as the elastic modulus, compressive strength, permeability, and bone ingrowth space of porous implants as input constraints, allowing the model to quickly deduce the optimal combination of pore shape, pore size, porosity, connectivity, and topological configuration. Zhang *et al.*[119] focused on four TPMS unit types—Primitive, FRD, IWP, and Gyroid—and used FEA to compute 8,000 sets of structural parameters and mechanical performance data. By combining genetic algorithms and setting a target modulus of 11.4 GPa, they determined parameters such as the periodic length (k) and the isosurface constant (C). Liu *et al.*[62] addressed the anisotropic mechanical properties of natural bone by using TPMS structures such as Gyroid and Primitive as subjects. They generated a stiffness matrix dataset through FEA and trained a BPNN to establish a high-precision mapping relationship. Combined with a regenerative genetic algorithm (RGA), this approach directly outputs the optimal structural parameters

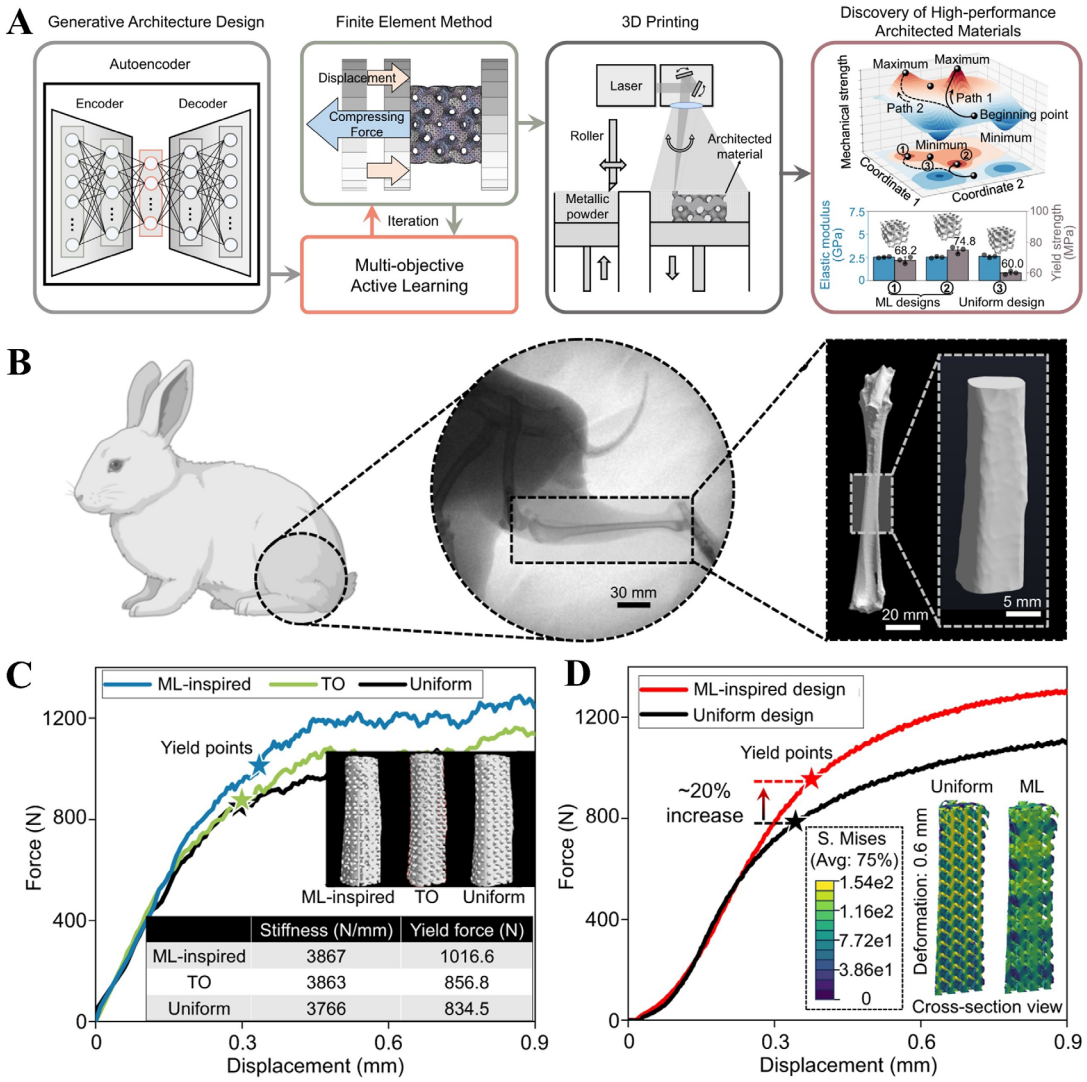

Figure 7. Heterogeneous porous scaffolds designed through the combination of machine learning and finite element analysis. (A) The design and manufacturing process of porous materials. (B) Bone defect in a New Zealand rabbit's middle part of the tibia. (C, D) The mechanical performance curves of heterogeneous topology structure and uniform structure. Reprinted with permission from Peng *et al.*[117] Copyright © 2023 Nature.

(porosity, unit arrangement ratio) based on the target bone stiffness. The final results showed an average error of less than 3% and a multi-objective error of less than 5%.

In summary, ML has demonstrated significant advantages in the configuration design of porous titanium alloy bone implants. ML can efficiently establish the mapping relationship between structure and performance from data, autonomously discover the optimal porous distribution patterns for mechanical properties, and achieve multi-objective collaborative optimization, including modulus matching, strength enhancement, stress uniformity, and favorable bone ingrowth, thereby substantially reducing the development cycle of implants.

However, there are certain challenges in the application of ML in the field of porous titanium alloys. Firstly, data quality and quantity are the primary bottlenecks constraining the performance of ML models. Each set of valid mechanical property data must be obtained through FEA or experimental preparation, and highly complex deep learning models inherently face the risk of overfitting. Moreover, in the field of AM, acquiring high-precision and noise-free data remains both costly and time-consuming. Secondly, ML models are often trained on a single TPMS topological type or a specific parameter range, resulting in limited generalization capabilities across different configurations and process conditions. In the future,

efforts should focus on data standardization, improving model generalization, and conducting engineering closed-loop verification as core strategies to advance ML from laboratory design to clinical applications.

3. Surface modification technology for additive manufacturing titanium alloy implants

Additive manufacturing (AM) technology offers unprecedented design flexibility for the personalized production of porous Ti alloy orthopedic implants. Nevertheless, the intrinsic layer-by-layer melting characteristics of processes such as LPBF and EBPBF result in high roughness and microscopic defects on the surface of the components. Such surface characteristics not only act as favorable locations for fatigue crack nucleation, thereby markedly lowering mechanical reliability, but may also trigger inflammatory responses *in vivo* due to the detachment of loose particles.[120,121] Consequently, post-surface treatment has become a critical step for the

Table 2. Different surface modification methods for porous titanium alloys by additive manufacturing

Modification technology	Modification method	Preparation principle	Advantages	Disadvantages	Applicable scene	Ref.
Mechanical modification	Sandblasting	Using compressed air, abrasive materials (Al_2O_3, TiO_2 particles) are sprayed at high speed onto the surface of the implant.	(i) Significantly improve surface roughness; (ii) Introduce residual compressive stress to enhance fatigue strength.	(i) Residual sandblasting particles cause inflammation; (ii) Difficult to deal with the internal pores of the porous structure.	Dental implants.	[123]
	Acid etching	The implant is immersed in a mixture of strong acids (HF, HNO_3, H_2SO_4) for corrosion	(i) Low cost; (ii) Construct micro/nano-scale surface textures.	It is difficult to independently control the large-scale roughness.	Internal cleaning of complex porous scaffolds and micro-texture construction.	[42]
	Sandblasting-acid etching	The large particles are sandblasted for roughening, followed by acid etching treatment.	Combining the macroscopic roughness of sandblasting and the microscopic texture of acid etching	The process steps are relatively complicated.	Dental implants, joint prosthesis bone-bone interface	[124]
Physical modification	Thermal spraying	Using a heat source to melt the coating material and then spraying it onto the substrate	(i) The coating is thick and has high bonding strength; (ii) The technology is mature and can produce wear-resistant coatings.	(i) It cannot cover the inner surface of the porous implant; (ii) High temperature may cause phase transformation of the matrix or decomposition of the coating.	The surface of a simple-shaped solid implant.	[125]
	PVD	Under vacuum conditions, the material is deposited on the substrate surface through evaporation or sputtering.	(i) The coating is dense and highly hard; (ii) Wear-resistant and corrosion-resistant; (iii) Precise control over coating thickness	The deposition rate is slow and the equipment is expensive.	The wear-resistant surface of the joint head.	[45]
Chemical modification	Hydrothermal	In a specially designed autoclave, chemical reactions are carried out using high-temperature and high-pressure aqueous solutions.	Suitable for AM complex porous structures, with uniform surface modification both inside and outside.	High-voltage equipment is required and the reaction process is quite lengthy.	Deep loading of the biological activation layer or antibacterial layer of the implant.	[126]

(*cont'd...*)

Table 2. (*Continued*)

Modification technology	Modification method	Preparation principle	Advantages	Disadvantages	Applicable scene	Ref.
	Alkali-heat treatment	The material is subjected to heat treatment after being soaked in strong alkali.	A bioactive titanate gel layer is formed on the titanium surface, inducing the generation of osteoid apatite.	The formed gel layer has relatively low mechanical strength and is prone to being scratched and falling off.	Surface activation of bone defect repair scaffolds.	[71]
	Sol-gel	The precursor undergoes hydrolysis and condensation to form a sol, and after coating, it is dried and sintered to form a coating.	(i) It is easy to incorporate functional elements (Ag, Cu, Sr); (ii) The processing temperature is relatively low.	(i) High drying shrinkage, prone to cracking; (ii) The coating is usually thin and has relatively weak adhesion to the substrate.	Porous scaffold drug sustained-release coating.	[127]
Electro-chemical modification	ECD	Under the influence of an electric field, the ions in the solution are reduced and deposited at the cathode.	The morphology and thickness of the coating can be precisely controlled by adjusting the current/voltage.	The bonding force between the coating and the substrate is usually not strong.	Preparation of antibacterial coating on the surface of porous scaffolds.	[128]
	Anodization	Using the sample as the anode, an oxide film is formed through oxidation in the electrolyte.	(i) TiO_2 nanotube arrays can be fabricated for drug loading; (ii) The bonding force between the oxide layer and the substrate is strong.	The oxide film is brittle and too thick, making it prone to cracking.	Local drug delivery system on the surface of implants.	[129]
	MAO	Under high voltage, the oxide film is broken down, resulting in micro-arc discharge, and the ceramic film is grown in situ.	(i) The formed ceramic membrane has high hardness, is wear-resistant and corrosion-resistant; (ii) The membrane layer is porous, which is conducive to the growth of cells; (iii) It is easy to incorporate bioactive elements from the electrolyte.	High energy consumption.	Construction of antimicrobial/bone-inducing dual-functional surfaces.	[24]

Abbreviations: AM: Additive manufacturing; ECD: Electrochemical deposition; MAO: Micro-arc oxidation; PVD: Physical vapor deposition.

clinical application of AM porous Ti alloy implants.[122] Table 2 outlines the preparation principles and advantages/drawbacks of various surface modification strategies.

3.1. Mechanical method

The mechanical surface modification methods have the advantages of mature technology and controllable cost, and can effectively improve the surface quality. These primarily include polishing,[130] sandblasting,[41] acid etching,[42] and sandblasting-acid (SLA) etching.[43,131] Mechanical polishing and electrolytic polishing achieve a shiny and smooth surface by directly removing surface particles.[130] Sandblasting employs high-speed jetting of hard particles (Al_2O_3) to impact the surface, effectively removing loose powder and creating uniform micron-scale pit-like morphology while introducing residual compressive stress to inhibit crack initiation. Bagehorn *et al.*[123] utilized sandblasting to increase the high-cycle fatigue strength of LPBF Ti_6Al_4V by approximately 20–30%, while achieving a surface roughness of 1–2 μm. This roughness range is considered ideal for maximizing osseointegration strength.[132] However, sandblasting has inherent limitations for porous structures, as the blasting medium struggles to reach deep internal pore surfaces, resulting in uneven treatment effects. It is only effective for external surfaces and shallow pores.[133] Acid etching treatment

dissolves the surface layer using strong acids, creating a multiscale morphology characterized by micron-scale pits superimposed with submicron-scale textures. This process significantly enhances hydrophilicity through surface hydroxylation, reducing the water contact angle from approximately 70° to around 40°.[134] More importantly, the acid can penetrate internal pores, achieving more uniform treatment compared to sandblasting. However, conditions must be strictly controlled to avoid excessive etching and hydrogen embrittlement risks. Chen *et al.*[42] effectively removed molten slag and constructed nanopores through multiple acid etching steps, forming a micro-nano composite structure that improves surface hardness and wear resistance. This modification strategy balances wear resistance with biocompatibility, making it suitable for medical bone implants.

SLA etching process combines the advantages of both techniques. It creates a multiscale hierarchical surface featuring 10–30 μm macro-pits overlaid with 1–3 μm micro-pits and submicron etching textures. This hierarchical structure is more in line with the natural morphology of bone matrix, simultaneously providing micron-scale anchor points for cell attachment and nanoscale signals to promote integrin clustering.[135] Zhang *et al.*[124] used SLA etching to treat the porous Ti_6Al_4V scaffold, as shown in Figure 8A. SLA etching reduced the surface roughness of the scaffold from 1.91 μm to 0.66 μm, increased the porosity from 54.5% to 61.6%, effectively restoring the designed pore structure and improving the efficiency of nutrient transport. Additionally, it significantly altered the surface wettability of the scaffolds.

In summary, sandblasting can rapidly create micro-scale roughness conducive to cellular proliferation but has limited effect on internal pores. Acid etching achieves uniform modification of both internal and external surfaces and enhances hydrophilicity. SLA etching has demonstrated superior osteogenic capabilities in both *in vitro* and *in vivo* studies.[136,137] Mechanical surface modification serves as the most fundamental experimental method, which is why many studies combine it with other techniques to develop functionally graded composite surface modification strategies.

3.2. Physical modification technology

Physical surface modification methods involve depositing functional coatings or altering the atomic structure of the surface layer without chemical reactions.[138,139] These techniques can significantly enhance the bioactivity, wear resistance, and antibacterial properties of implants while preserving the structural integrity of the material.[140] Among them, thermal spraying and physical vapor deposition (PVD) are several major surface modification technologies.[141,142]

Thermal spraying technology involves melting or semi-melting coating materials using a high-temperature heat source and then depositing them onto the substrate surface at high speed. Among these techniques, plasma-sprayed hydroxyapatite (HA) coatings have been widely used in clinical hip joint prosthesis. Heimann[125] noted that plasma-sprayed HA coatings (with a thickness of 50–150 μm) significantly promote osteoblast adhesion and mineralization. Clinical follow-up studies have shown that the 10-year survival rate of the prosthesis exceeds 95%. However, conventional plasma spraying faces challenges such as uneven coating crystallinity, limited interfacial bonding strength (15–30 MPa), and HA decomposition caused by high temperatures.

PVD technology deposits atoms from a target material onto a substrate surface via physical mechanisms such as sputtering, evaporation, or ion plating in a vacuum environment, enabling the fabrication of dense thin-film coatings with thicknesses ranging from nanometre to micrometre.[143] Among various PVD approaches, magnetron sputtering is the most extensively employed method, which can synthesize hard coatings such as TiN and Tio_2. while also allowing for the incorporation of bioactive elements like Cu and Ag. These coatings significantly enhance surface hardness, wear resistance, and antibacterial properties.[144] Diez-Escudero *et al.*[143] utilized arc PVD technology to deposit a TiAgN composite coating on the surface of porous Ti6Al4V trabecular scaffolds fabricated via EBPBF, as shown in Figure 8B. The coating sustainably releases Ag^{2+}, significantly inhibiting the adhesion, proliferation, and biofilm formation of *Staphylococcus aureus* and *Staphylococcus epidermidis*.

Physical surface modification techniques preserve the excellent mechanical strength of Ti alloys without altering their bulk composition. By controlling the surface microstructure and introducing bioactive elements, a dense nanoscale bioactive layer is formed, significantly enhancing the osseointegration capability, antibacterial performance, and wear resistance of Ti alloys. However, the particle transmission paths in physical methods such as thermal spraying and magnetron sputtering are prone to obstruction by pore walls, resulting in uneven coverage of the inner surface of the pores.

3.3. Chemical modification technology

Chemical surface modification method generates functional coatings through *in situ* chemical reactions in solution, thereby altering the chemical composition of the surface layer.[145] These methods offer advantages such

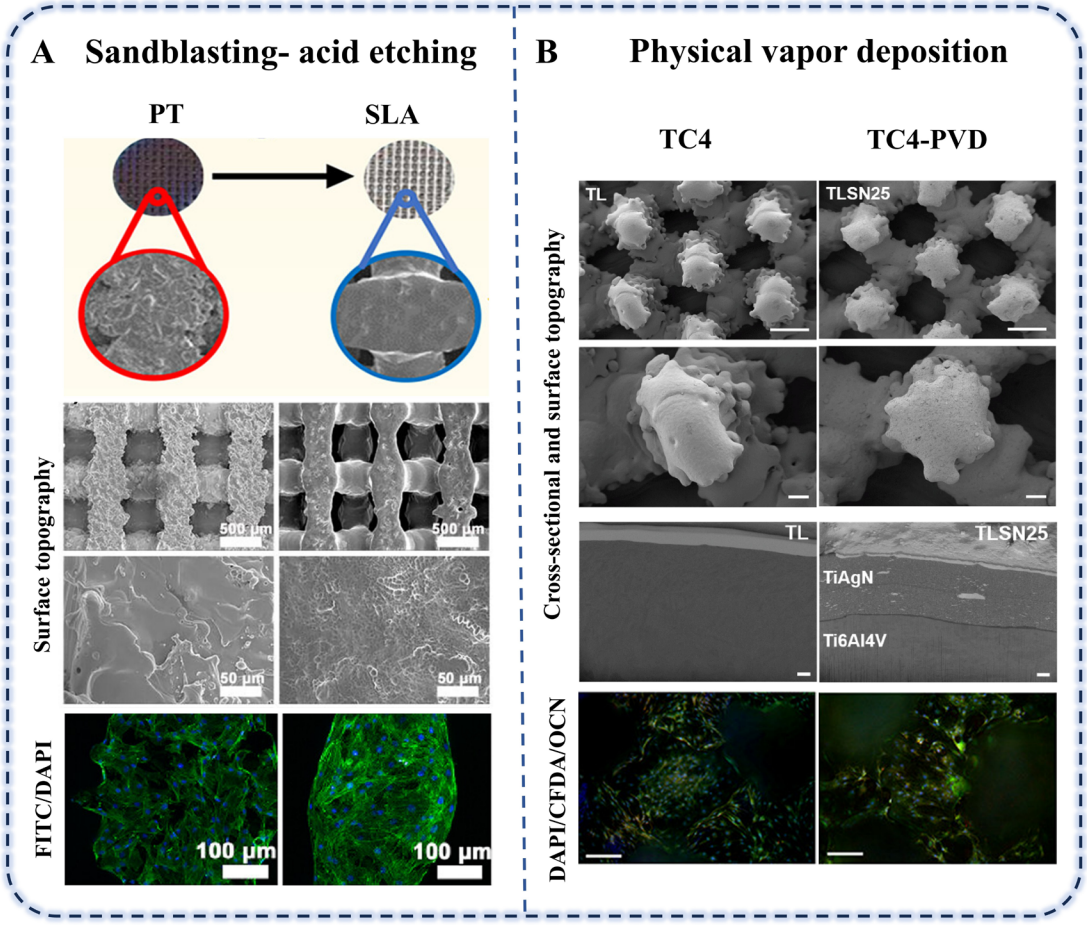

Figure 8. Surface modification techniques for porous titanium alloys. (A) The surface morphology and biocompatibility of titanium alloy scaffolds subjected to sandblasting-acid etching treatment. Reprinted with permission from Zhang *et al.*[124] Copyright © 2023 American Chemical Society. (B) The cross-sectional, surface morphology and biocompatibility of titanium alloy scaffolds subjected to physical vapor deposition (PVD) method. Reprinted with permission from Diez-Escudero *et al.*[143] Copyright © 2022 American Chemical Society.

as mild processing conditions, the ability to treat complex porous struct'res' inner surfaces, and relatively low costs. Hydrothermal treatment involves growing functional coatings in a high-temperature and high-pressure aqueous solution environment. This process can produce oxide or phosphate layers with high crystallinity and strong bonding to the substrate.[146] Compared to conventional chemical treatments under atmospheric pressure, hydrothermal conditions (typically 120–200 °C, saturated vapor pressure) significantly enhance reaction activity and coating density.[147] For instance, Wu *et al.*[148] used oyster shells as the calcium source and carried out hydrothermal treatment (at 150 °C for 1 h) to synthesize a coating containing beneficial trace elements (sodium, magnesium, strontium) and AB-type carbonate. The surface presented a mixed morphology of nanorods and ellipsoids, which showed excellent adhesion and proliferation effects on human osteoblasts. In the study of osteogenic functional coatings, Zhou *et al.*[126] developed a modified hydrothermal method (190 °C, 8 h) to prepare a $CaHPO_4$ coating on AM porous Ti_6Al_4V scaffolds. This coating sustainably released Ca^{2+} and exerted bone immunomodulatory functions by inducing macrophage polarization toward the M2, significantly enhancing new bone formation in a rat femoral defect model. Alkali-heat treatment is based on the principle that when titanium alloys are immersed in high-concentration NaOH or KOH solutions, which leads to the formation of a hydrated titanate gel layer rich in Ti-O-Na/ Ti-O-K bonds on the surface. Subsequent heat treatment converts this layer into an amorphous or microcrystalline sodium titanate/ kalium titanate layer. This surface layer can induce bone-like HA deposition in simulated body fluid, thereby conferring bioactivity to the surface.[149,150] Luo *et al.*[151] adopted a combined process of HCl pretreatment,

NaOH alkali-heat treatment and high-temperature curing to prepare sodium titanate ($Na_2Ti_6O_{13}$) nanowire cluster coatings on LPBF-produced porous Ti_6Al_4V surfaces. The contact angle of the 48-hour treatment group was as low as 5°. Within 7 days in simulated body fluid, a 15-μm-thick apatite layer could be formed, and the compressive strength of the material still met the mechanical requirements of cortical bone. Lei *et al.*[71] constructed a bioactive sodium titanate coating on porous Ti_6Al_4V pedicle screws through acid etching pretreatment and alkali-heat activation, as shown in Figure 9A. Alkali-heat treatment introduced a large number of hydroxyl groups and Na^+ active sites on the material surface, resulting in a more negative Zeta potential, which can enrich positively charged proteins such as fibronectin and collagen through electrostatic interactions. This coating significantly enhances surface hydrophilicity and surface energy, providing an ideal interface for cell adhesion and osseointegration. Hydrothermal and alkali-thermal techniques, as low-cost and highly adaptable surface modification methods, can construct uniform and strongly bonded bioactive coatings on complex porous titanium surfaces. This enables multi-level optimization, including defect removal, surface activation, osteoinduction, and enhanced fixation. Such processes do not damage the porous structure or compromise mechanical properties.

The sol-gel method prepares colloidal solutions through the hydrolysis and polycondensation of metal salts or inorganic salts, followed by deposition onto substrates via techniques such as dip-coating, spin-coating, or dip-drawing.[152,153] This method offers precise control over coating composition and relatively low processing temperatures. Dong *et al.*[154] deposited a polydopamine transition layer on the surface of the porous titanium scaffold, and then *in situ* formed a hydrogel composite coating loaded with Mg^{2+} and ZIF-8 nanoparticles through the Schiff base reaction. This method enables uniform coating of the gel layer without blocking the pores, and Mg^{2+} and Zn^{2+} can achieve stable and sustained release for more than 30 days. In terms of imparting antibacterial function, the sol-gel method can be combined with drug-loaded hydrogels to construct sustained-release drug delivery systems. Huang *et al.*[127] loaded vancomycin/chitosan-hyaluronic acid hydrogels onto AM porous Ti-10Ta-2Nb-2Zr scaffolds (modified by MAO), achieving sustained drug release for over 35 days. The 2.5 wt.% vancomycin-loaded group maintained antibacterial activity without inhibiting osteoblast proliferation and differentiation, as shown in Figure 9B. Ma *et al.*[155] further developed an intelligent responsive antibacterial coating by constructing a vancomycin/thermosensitive hydrogel/polycaprolactone film composite system on the surface of AM porous Ti alloy rods. The polycaprolactone outer membrane could be degraded by bacterial lipases to trigger drug release, enabling intelligent response to release drugs only when the wound was infected. *In vivo* experiments confirmed that this coating effectively prevented *S. aureus* infections while preserving osteointegration capability. Sol-gel composite modification serves as an efficient method for surface functionalization of porous implants. Its main advantages include the ability to deeply coat bioactive particles within pores, with controllable composition and release. This approach can simultaneously address issues such as insufficient osseointegration and infection in the clinical application of porous titanium.

In summary, the hydrothermal method can produce functional coatings with high crystallinity and strong bonding to the substrate, and the reaction conditions are controllable, making it suitable for uniform modification of porous structures. The alkali-heat treatment process is mature and can form a bioactive layer with HA induction ability, though the resulting coatings are relatively thin and require high-temperature post-treatment. The sol-gel method provides flexible compositional control, enabling the preparation of multi-component composite coatings. However, the uniform coverage of the coating on the high aspect ratio pores requires assistance from technologies such as vacuum. Chemical surface modification technologies create multi-element and multifunctional surface modification layers, providing a flexible technical route to enhance the corrosion resistance, antibacterial properties, and osteogenic performance of AM Ti alloy implants.

3.4. Electrochemical method

Electrochemical surface modification methods generate functional oxide layers on Ti alloy surfaces through electric field-driven oxidation reactions, offering advantages such as strong coating-substrate adhesion, uniform treatment of complex porous structures, and excellent controllability of process parameters. Electrochemical deposition (ECD), anodization, and MAO have been widely investigated as effective surface modification techniques for AM porous Ti alloy implants.[156-158]

ECD utilizes an electric field to drive ions or charged particles in a solution to deposit as a film on the electrode surface, enabling the preparation of HA, calcium phosphate, and other coatings at relatively low temperatures. This technology has been successfully applied to the surfaces of AM materials to produce various functional coatings. Chudinova *et al.*[128] employed an electrophoretic deposition process to deposit calcium phosphate nanoparticles (CaPNPs, particle size ~90 nm) on the surface of

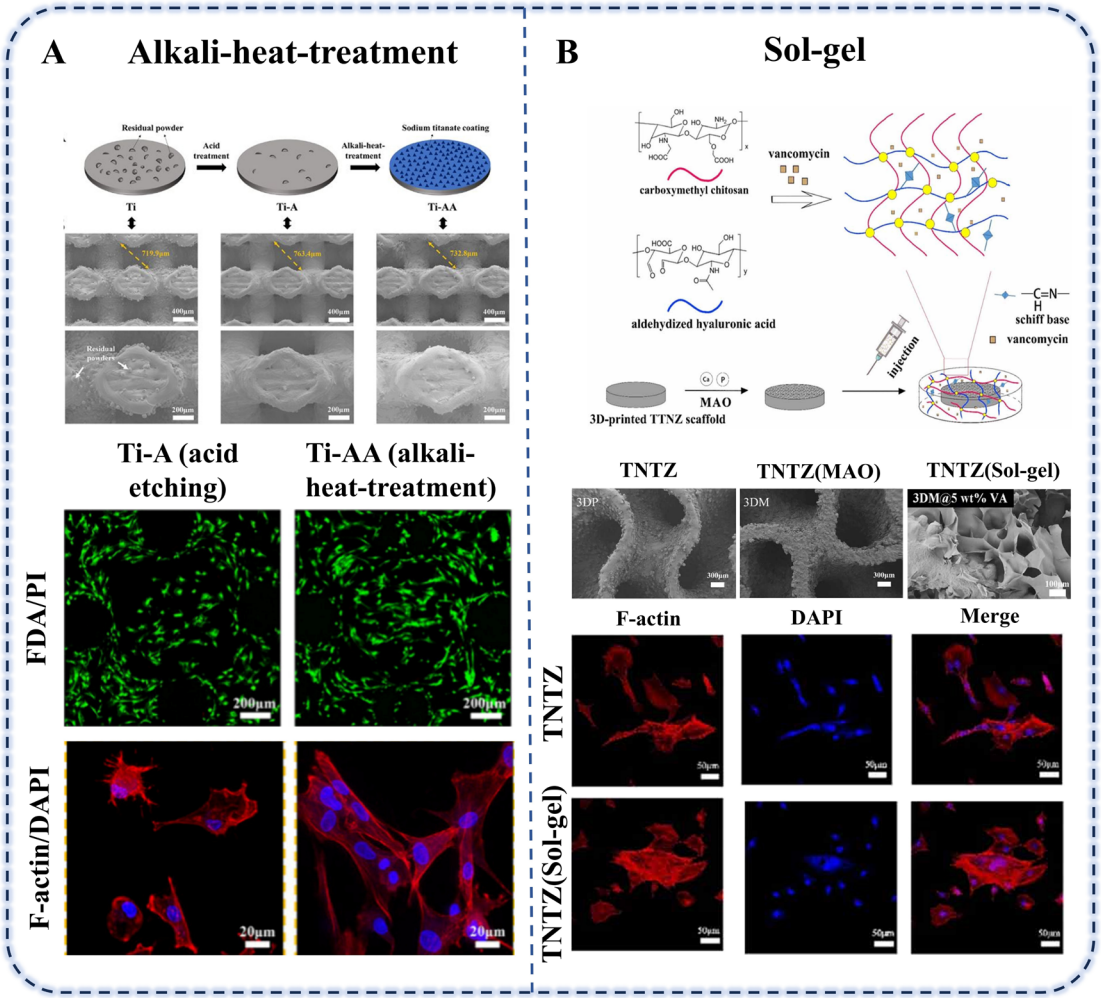

Figure 9. Chemical modification technology techniques for porous titanium alloys. (A) The morphology and cell activity of titanium alloy scaffolds subjected to alkaline heat treatment. Reprinted with permission from Lei *et al.*[71] Copyright © 2025 American Chemical Society. (B) Schematic diagram of sol-gel method and microscopic morphology biocompatibility of the scaffold. Reprinted with permission from Huang *et al.*[127] Copyright © 2022 IOPscience.

porous Ti_6Al_4V scaffolds fabricated by EBPBF. This coating effectively promoted osteogenic differentiation by mimicking the composition of bone minerals and rendered the scaffold surface superhydrophobic. Fan *et al.*[159] further utilized ECP to prepare cerium oxide nanoparticle coatings on the surface of AM porous Ti_6Al_4V scaffolds. The Ce existed in mixed valence states, endowing the coating with antioxidant activity. This coating not only upregulated the expression of osteogenesis-related genes (*ALP*, *OCN*, *COL1*) but also modulated the inflammatory microenvironment by increasing the expression of anti-inflammatory genes (*ARG1*, *IL10*) and decreasing the expression of pro-inflammatory genes (*iNOS*, *TNFa*). Wei *et al.*[160] proposed an innovative strategy involving electrophoretic deposition to construct a carbon nanotube buffer layer and a mesoporous silica nanoparticle functional layer on Ti_6Al_4V scaffolds, loaded with mechano-growth factor. *In vivo* experiments showed that skeletal muscle cells accounted for 58.68% of the tissue, significantly higher than the 25.88% observed in the pure Ti group. The maximum avulsion force of muscle attachment reached 31.17 N/cm, and the implant regulated macrophage polarization toward the M2 phenotype to alleviate inflammatory responses.

Anodization can be used to fabricate highly ordered TiO_2 nanotube arrays in fluorine-containing electrolytes. The diameters and lengths of the nanotubes can be controlled by adjusting the voltage, time and composition of the electrolyte. This nanotubular structure significantly enhances the surface-specific area and hydrophilicity, providing a favorable nano-topological environment for cell adhesion, while the hollow tubular cavities serve as storage reservoirs for drugs or growth factors, enabling

localized sustained release.[161] Gunputh *et al.*[162] anchored Ag nanoparticles onto nanotube surfaces via *in situ* growth, achieving over 80% bactericidal efficiency. Their innovation involved further sintering nano-HA as a top coating, which preserved antibacterial efficacy while enabling slow Ag release (3.27 ± 0.15 μg/L over 24 hours), balancing antimicrobial with biocompatibility. Yang *et al.*[163] innovatively adopted a Mg^{2+} doping strategy. They prepared TiO_2 nanotubes (TNTs) with a diameter of 80 nm and a length of 2 μm through anodization, followed by Mg^{2+} doping via a hydrothermal method. The sustained release of Mg^{2+} demonstrated significant antibacterial effects against various bacteria, while also inhibiting osteoclastogenesis by downregulating the NF-κB/NFATc1 signaling pathway. Anodization can also be utilized to construct drug/ion-loaded functionalized surfaces. He *et al.*[164] developed a hierarchical drug delivery system using TiO_2 nanotubes as carriers. They fabricated nanotubes (~110 nm in diameter) on the surface of LPBF-produced porous Ti scaffolds, loading with 1α,25-dihydroxyvitamin D_3 (VD_3), and constructing thermosensitive Pluronic F-127 hydrogel for controlled drug release. This system achieves an ideal sustained-release profile of VD_3, with a cumulative release rate of 80% within 14 days. *In vitro* experiments demonstrated significant upregulation of osteogenic genes (*ALP*, *COLI*, *RUNX2*) in MC3T3-E1 cells. In the *in vivo* rabbit femoral implant experiment, the new bone formation rate after 2 weeks was 66.5% higher than that of the porous Ti scaffold without drug loading, and the bone-implant contact rate reached 40.8%, providing an effective solution for accelerating early bone integration.

MAO is a process that generates porous ceramic coatings *in situ* on Ti alloy surfaces through micro-arc discharge under high voltage (200–600 V). The coating thickness can reach 5–30 μm, and its bonding strength is significantly superior to that of sprayed or sol-gel coatings.[21,22] By adjusting the electrolyte composition, bioactive elements such as Ca, P, Sr, and Mg can be incorporated into the coating, endowing it with excellent HA induction capability and osteogenic activity.[24,52,165,166] To address the specific needs of osteoporosis patients, Kołodziejska *et al.*[167] developed an MAO coating doped with Sr^{2+}. The Sr^{2+} achieve bidirectional regulation of bone metabolism via the CaSR receptor, simultaneously promoting osteoblast differentiation and inhibiting osteoclast activity. Li *et al.*[168] systematically compared the effects of silicate, phosphate, and mixed electrolytes on coating growth mechanisms. The study revealed that silicate-based coatings grew outward, exhibiting excellent wear resistance but poor adhesion. The phosphate-based coatings grew inward, showing superior adhesion but insufficient wear resistance. The mixed electrolytes achieved a balanced performance. AM Ti alloy implants feature customizable complex structures, and MAO technology is not affected by material structure.[169,170] Chen *et al.*[171] addressed the issue of pedicle screw loosening in spinal fusion surgery by combining LPBF with MAO to fabricate Ti_6Al_4V screws with fully interconnected porous structures. Through systematic optimization of oxidation time (3/5 min) and voltage (300/400 V), they obtained porous coatings (pore size 300–1200 nm) rich in bioactive ions such as Ca, Si, and P. *In vitro* and *in vivo* experiments confirmed that the Ti@MAO-3-300 group exhibited bone maturity and pull-out strength eight times higher than conventional screws. Yang *et al.*[172] innovatively employed low-modulus porous β-type Ti2448 alloy combined with MAO treatment to produce an immunomodulatory coating, as shown in Figure 10. This coating, enriched with bioactive components such as Nb_2O_5 and SnO_2, which could induce macrophage polarization toward the M2 phenotype and promote bone regeneration, demonstrating the synergistic advantages of material design and surface modification.

In summary, the inherent solution-phase reaction characteristics of electrochemical methods enable them to effectively treat the inner surfaces of complex porous structures. This capability allows for the construction of functional coatings on the surfaces of biomedical porous Ti alloy implants, endowing them with excellent bioactivity, antibacterial properties. The anodization process can generate a uniform and dense nanoscale TiO_2 film on the surface of porous titanium alloys. These nanochannels can increase surface roughness and hydrophilicity, providing sites for bone cell adhesion. Additionally, by doping the electrolyte with Ca^{2+} and P^{2+}, the surface can be endowed with preliminary bioactivity, inducing hydroxyapatite deposition. MAO produces a ceramic oxide film that grows *in situ* on the titanium alloy surface through high-voltage micro-arc discharge. This film exhibits far superior bonding strength, hardness, and wear resistance compared to anodized films, thereby enhancing the long-term service stability of implants. The hierarchical microporous structure formed on its surface is more compatible with the growth habits of bone cells. However, in the face of the high demands of clinical applications for bone implants, relying solely on a single anodization or MAO technology makes it difficult to achieve functions such as anti-inflammatory properties, drug sustained release, and photothermal responsiveness. In the future, it will be necessary to combine with other surface modification technologies to form multifunctional composite coatings, thereby achieving more ideal enhanced osseointegration effects.

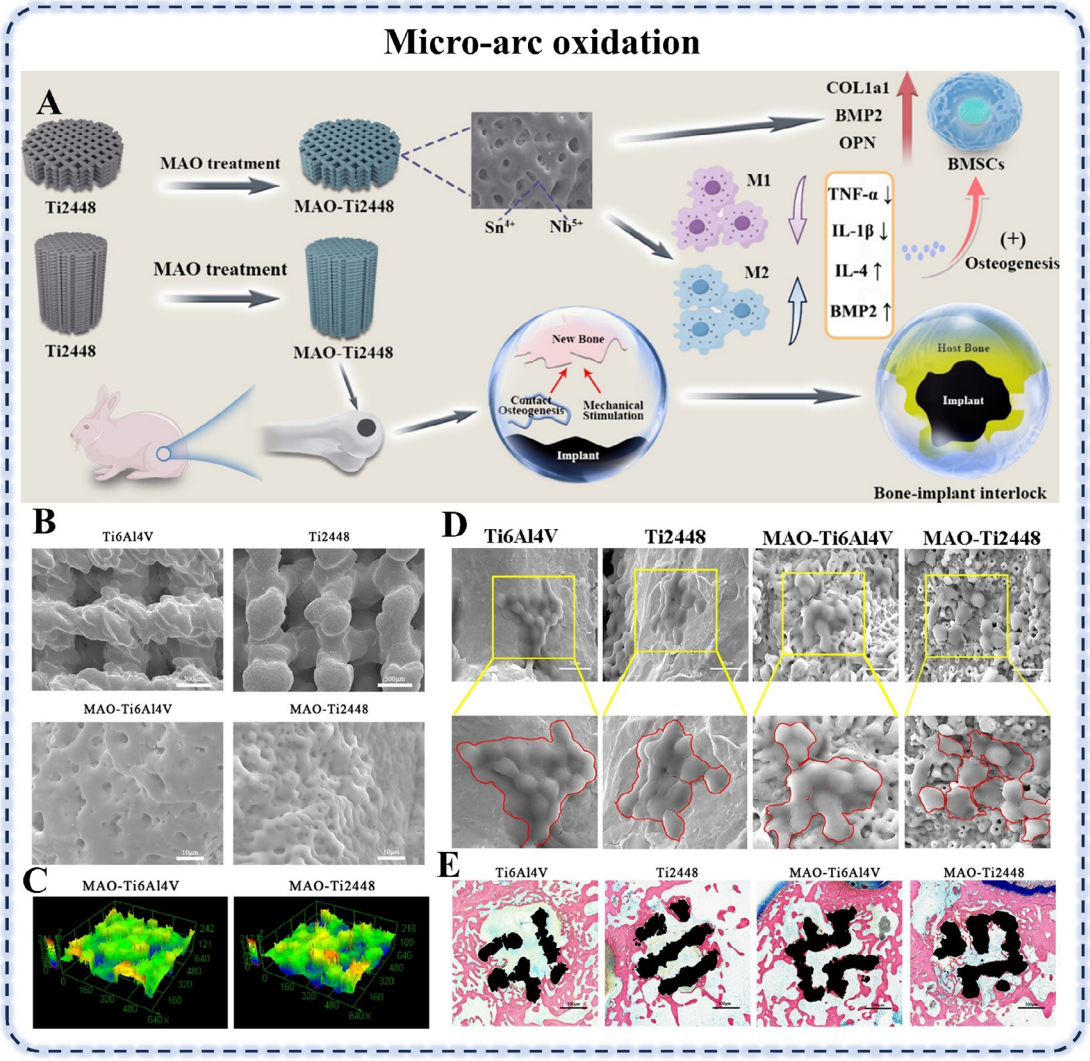

Figure 10. Fabrication of Nb_2O_5 and SnO_2 coatings on β-titanium alloy surfaces via MAO technology. (A) Schematic diagram of the biological experiment of MAO-Ti2448. (B) Surface morphology. (C) Surface roughness of the coatings. (D) Morphology of macrophages. (E) Bone tissue metrological analysis. Reprinted with permission from Yang *et al.*[172] Copyright © 2024 American Chemical Society.

3.5. New multifunctional composite surface modification technology

Traditional surface modification techniques, which aim to enhance hydrophilicity, improve osseointegration, and provide antibacterial properties, often exhibit limited functionality and struggle to meet the current high demands for multifunctional integration on bone implant surfaces. In recent years, the development of stimulus-responsive smart surfaces has emerged as a cutting-edge direction in implant surface engineering. The core concept lies in endowing implants with the ability to perceive and respond to specific endogenous or exogenous signals.[173] In terms of endogenous stimuli, pH-sensitive coatings can undergo chemical bond cleavage or protonation-induced swelling in the acidic environment resulting from bacterial infection, thereby accelerating the release of loaded antibacterial agents or metal ions.[54] Peptide enzyme-responsive coatings, triggered by osteoclast activity during bone remodeling, demonstrate significant anti-biofilm activity, enabling effective growth of osteoblasts and fibroblasts.[174] Regarding exogenous stimuli, near-infrared photothermal-responsive coatings enable localized and controllable temperature increases under near-infrared irradiation. This mechanism utilizes physical thermal damage to eliminate pathogens, including drug-resistant bacteria and mature biofilms, thereby circumventing

the limitations of antibiotic resistance associated with traditional approaches.[175,176] Chen *et al.*[177] fabricated a hydrogel coating with vertically gradient micropores via *in situ* polymerization and incorporated monolayer MoS_2 nanosheets to endow the coating with photothermal conversion capability. The coating exhibited a high bonding strength of 480 kPa with the Ti6Al4V substrate, and the MoS_2 achieved a bactericidal rate exceeding 99% against both *Escherichia coli* and *S. aureus* under photothermal effects. Wang *et al.*[178] developed a tannic acid-based photothermal-responsive hydrogel coating by integrating Prussian blue (PB) nanoparticles, quercetin (QUE), osteogenic growth peptide (OGP), and stromal cell-derived factor 1α (SDF-1α) into the hydrogel, which was then spin-coated onto the surface of Ti6Al4V scaffolds. Under photothermal conditions, this modified layer enhanced molecular mobility and drug release efficiency, while suppressing SASP inflammatory factors and inducing macrophage polarization toward the M2 phenotype to exert anti-inflammatory effects. Meanwhile, the release of OGP and SDF-1α activated the Wnt/β-catenin pathway, promoting osteogenic differentiation of bone marrow mesenchymal stromal cells (BMSCs). In addition, piezoelectric-responsive surface coatings loaded with $BaTiO_3$ and ZnO nanoarrays can convert periodic mechanical loads generated by daily human movements into surface microelectrical signals. These signals mimic endogenous bioelectric potentials to promote osteoblast proliferation, differentiation, and bone mineralization deposition, enabling self-powered bone repair without the need for external energy input.[55] Chen *et al.*[179] grew $BaTiO_3$ nano coating *in situ* on the surface of a Ti6Al4V scaffold via hydrothermal synthesis, followed by polydopamine chemical deposition to stably anchor vancomycin-loaded lipid microbubbles onto the scaffold surface. Under low-intensity pulsed ultrasound (LIPUS) stimulation, the $BaTiO_3$ coating generates a stable microcurrent, which triggers the rupture of the lipid microbubbles and subsequent drug release. This coating enables controlled drug release in an infected microenvironment.

Additionally, drug sustained-release coatings represent another important direction for the surface functionalization of porous bone implants. Controlled drug release systems can provide continuous stimulation to promote bone regeneration. Traditional surface modification techniques often rely on introducing a large number of pores for drug loading. However, drugs are physically mixed into porous implants as free particles without constraints, they often suffer from burst release issues. Luo *et al.*[180] pre-modified Ti6Al4V scaffolds with a polydopamine surface coating. They then prepared double-network hydrogel microspheres using microfluidic technology to encapsulate hypoxia-induced human umbilical vein endothelial cell-derived exosomes (HExo). These microspheres were subsequently immobilized on the polydopamine-modified titanium scaffold surface through covalent bonding and physical anchoring. The hydrogel microspheres achieved sustained release of HExo over a period of up to 18 days. The continuously released HExo activated the MAPK, mTOR, HIF-1, and VEGF signaling pathways, simultaneously upregulating the expression of genes related to osteogenesis (*ALP*, *OCN*, *RUNX2*) and angiogenesis (*VEGF*, *CD31*). Che *et al.*[181] constructed a dual-carrier sequential drug release coating on the surface of a titanium alloy porous scaffold. They used a thermosensitive collagen hydrogel as a rapid-release carrier to encapsulate the immunomodulator 4-octyl itaconate (4-OI), and employed ZIF-8 nanoparticles as a sustained-release carrier to encapsulate the osteogenic factor BMP-9, as shown in Figure 11. This composite coating achieved precise sequential release of anti-inflammatory and osteogenic factors. In the first phase, the burst release of 4-OI inhibited the NF-κB signaling pathway, rapidly controlling local inflammation. In the second phase, the sustained release of BMP-9 promoted the osteogenic differentiation of BMSCs.

Stimulus-responsive coatings and drug-release coatings have demonstrated significant potential in the functionalization of porous bone implant surfaces. Both *in vitro* and *in vivo* studies have preliminarily confirmed the remarkable anti-inflammatory and osteogenic capabilities of these functionalized scaffolds. However, due to the innovative nature of such surface modification strategies and the lack of unified *in vitro* and *in vivo* evaluation standards, challenges remain in terms of long-term safety and stability in clinical translation.

4. Application of additive manufacturing titanium alloy bone implants

With the widespread adoption of precision medicine, traditional standardized implants have gradually revealed limitations in addressing complex bone defects, repairs in special anatomical regions, and long-term functional maintenance. These challenges include poor anatomical matching, significant stress shielding effects, and insufficient interfacial bonding. AM technology offers a revolutionary solution by constructing biomimetic porous structures and personalized geometries, along with advanced surface modification techniques.[3,182]

4.1. Orthopedic implants and joint prosthesis

In clinical practice, the core advantage of AM technology lies in its ability to design materials based on patient CT

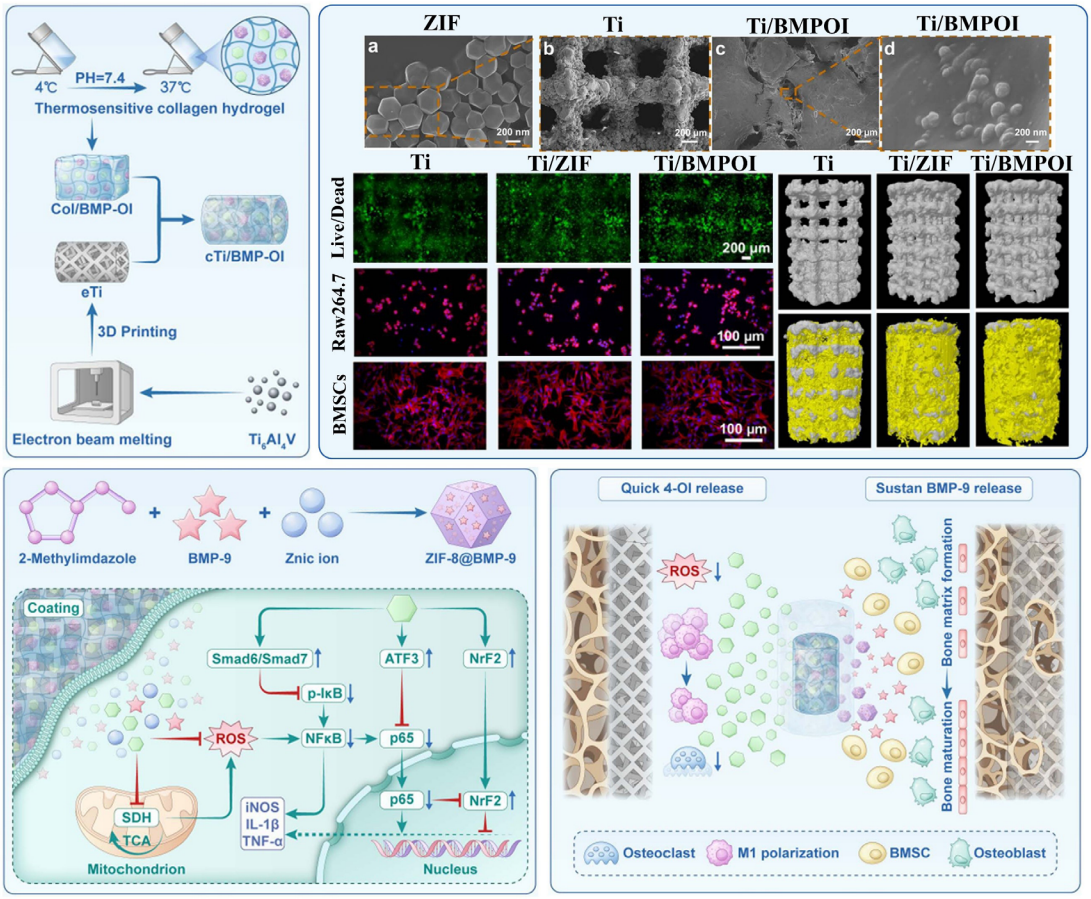

Figure 11. Synthesis schematic diagram, microscopic morphology, cell activity, and bone integration mechanism diagram for Ti/BMPOI. Reprinted with permission from Che *et al.*[181] Copyright © 2026 Ivyspring International.

imaging data, significantly improving the anatomical matching between implants and human bones.[183] This is particularly critical in complex bone tumor resection, joint replacement, and spinal orthopaedic surgeries,[63,184,185] as shown in Figure 12. For the anatomically complex pelvic region, Xu *et al.*[186] demonstrated the superiority of 3D-printed prostheses. Twenty pelvic tumour patients were divided into a 3D-printed group and a conventional materials group for comparison. The surgical indicators, the negative rate of tumour resection margins, and the MSTS functional score were evaluated. The results showed that the average incision length (10.0 ± 3.1 cm), operation time (115.2 ± 25.3 min), and intraoperative blood loss (213.2 ± 104.6 mL) in the 3D-printed group were significantly lower than those in the traditional materials group. However, the negative rate of tumour resection margins (90%) and the MSTS score (23.8 ± 1.3) in the 3D-printed group were significantly higher ($p < 0.05$). This process precisely models the preoperative CT data to achieve anatomical matching between the prosthesis and the bone defect. Compared with traditional screw-rod/plate fixation, the porous structure promotes bone ingrowth, reduces surgical trauma, and improves the accuracy of tumour resection, significantly improving postoperative functional recovery. In the field of spinal surgery, Siu *et al.*[187] reported a case using EBPBF technology to fabricate customized Ti_6Al_4V intervertebral fusion device for the treatment of osteoporotic spinal deformities. The tailored implant perfectly matched the vertebrae, effectively preventing subsidence and displacement due to osteoporosis. Postoperative imaging confirmed excellent spinal sequence recovery and bone fusion. This solution addressed the challenge of standard fusion devices being difficult to adapt to the diseased vertebrae. For fine reconstruction of limb and craniofacial joints, personalized techniques also demonstrate great potential. Cheng *et al.*[188] utilized the mirroring principle of the healthy part to design and manufacture Ti alloy prostheses for distal fibular and lateral malleolar. Two-year follow-ups revealed that the patient's ankle joint function was close to normal, proving

the feasibility of Ti alloy prostheses in replacing complex joint structures. Sharma *et al.*[189] developed a Ti alloy prosthesis for the temporomandibular joint using selective laser sintering (SLS), with a yield strength of 990 MPa, a tensile strength of 1045 MPa, and a surface roughness of 50.2 μm. After stress relief treatment at 800 °C in an argon atmosphere, dimensional accuracy reached ±50 μm. Compared to commercial standardized prostheses, this method achieved precise anatomical matching with mandibular structures. The high specific strength and biocompatibility of AM Ti alloy minimized postoperative loosening, shortened operation time, and reduced the risks of infection, overcoming the poor adaptability of traditional prostheses in complex curved surfaces of the mandibular region. Furthermore, for extremely small phalangeal defects, Bregoli *et al.*[190] demonstrated that even miniaturized Ti alloy implants with diameters as small as 1.5 mm, after being prepared by LPBF and subjected to shot peening, could provide sufficient torsional strength (11.1 ± 0.6 Nm) and axial retention force (437.5 ± 11.5 N). The biocompatibility and porous structure synergistically enhanced implant fixation stability, restoring over 50% of hand function.

However, morphological matching is insufficient to address the long-term stability of implants. The stress-shielding effect caused by the significantly higher elastic modulus of Ti alloys (approximately 110 GPa) compared to human bone is a primary reason for prosthetic loosening. Therefore, biomechanical design has become the key to technological breakthrough. Zhang *et al.*[191] tackled the issue at the material level by employing LPBF to fabricate a β-type Ti24Nb4Zr8Sn alloy. Its elastic modulus was as low

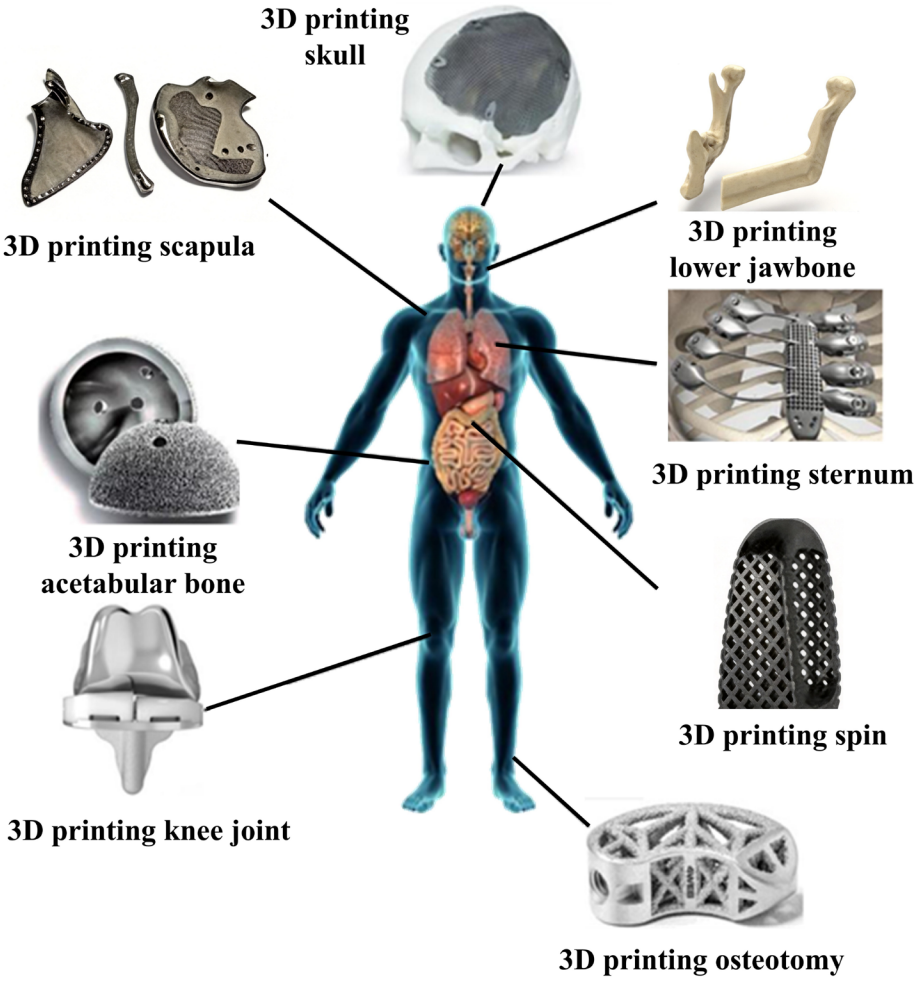

Figure 12. The application of additive manufacturing in orthopedic implants. Reprinted with permission from Sun & Shang.[63] Copyright © 2020 Scientific research.

as 53 GPa, while maintaining a tensile strength of 665 MPa, achieving better mechanical compatibility with bone tissue. Other studies have focused on structural innovations. Li *et al.*[192] designed a gradient porous Ti_6Al_4V scaffold based on TPMS to simulate the gradient mechanical properties of natural bone. By varying pore sizes from 100 to 700 μm, they achieved a continuously adjustable compressive modulus ranging from 3.07 to 7.33 GPa. The *in vivo* implantation experiment in pigs showed that the bone volume/total volume reached 12.84% after 5 weeks, significantly higher than the 3.28% in control group. Rana *et al.*[193] introduced a more innovative negative Poisson's ratio structure and used the SLS process to fabricate heterogeneous porous Ti femoral stems. Based on CT data, they optimized the pore distribution and tested the stress shielding rate and mechanical compatibility. Results showed that the optimized implant reduced the average stress shielding rate from 56% to 18%, with significantly less bone resorption in Gruen zones. Compared to solid Ti prostheses, this heterogeneous structure synergistically modulates stress distribution and enhances long-term prosthetic stability through porosity and negative Poisson's ratio effects.

Although AM technology has endowed the implants with structural advantages and mechanical compatibility, their original fabricated surfaces often exhibit issues such as high roughness, insufficient bioactivity, or lack of antibacterial ability. Therefore, surface modification has become an essential step in optimizing implant performance. Chowdhury *et al.*[194] systematically reviewed post-processing techniques such as laser treatment, electrochemical polishing, chemical etching, heat treatment, and surface coatings in the fabrication of Ti alloy implants using LPBF/EBPBF. They also evaluated the effects of each technique on the physical properties, mechanical properties, tribological characteristics, and biological responses of the implants. The results demonstrated that laser polishing reduced the surface roughness of Ti_6Al_4V samples from 14.21 μm to 1.71 μm while enhancing fatigue strength. MAO formed a microporous oxide coating on complex structural surfaces, reducing the elastic modulus and improving osseointegration. HA coatings, prepared via plasma spraying or sol-gel methods, significantly enhanced bioactivity. Compared to untreated AM implants, the samples after surface functionalization exhibited improvements in antibacterial properties, osteoconductivity, and mechanical compatibility. Notably, lattice structure implants combined with surface coating technology effectively alleviated stress shielding, achieving synergistic optimization of mechanical and biological performance. The review by Li *et al.*[195] further highlighted that post-processing techniques such as sandblasting, HA coating, and MAO could enhance the osseointegration efficiency of Ti alloys. By introducing antibacterial elements like Cu and Ag and combining with the porous structure design of AM, these methods simultaneously improved the implants' mechanical adaptability, osseointegration capacity, and antibacterial properties.

In summary, the personalized customization of AM Ti alloy has addressed the challenge of morphological matching in complex anatomical regions, significantly enhancing surgical precision and postoperative functionality. The gradient porous structure design effectively mitigates stress shielding effects, improving the long-term stability of implants. Surface modification techniques endow implants with multiple biological functions, including antibacterial properties, osteogenesis promotion and soft tissue integration. With continuous optimization of printing processes and innovations in surface modification technologies, AM Ti alloy implants have demonstrated unparalleled advantages over traditional implants across various fields, such as joint replacement, spinal fusion, pelvic reconstruction, and mandibular repair.

4.2. Dental implant

The deep integration of AM technology with Ti alloy materials is reshaping the technological of dental implants, fundamentally addressing long-standing limitations of traditional dental implants in mechanical compatibility, bioactivity, manufacturing precision, and personalized customization. In order to enhance the biomechanical performance and bone integration rate of dental implants, in recent years, some scholars have innovatively incorporated porous structures into the design of dental implants, aiming to reduce the overall elastic modulus of the implants and alleviate the mismatch in mechanical properties between the implants and the surrounding bone tissues.[196] To address the insufficient fatigue strength of traditional porous Ti_6Al_4V dental implants. Xiong *et al.*[197] employed LPBF to design and fabricate porous Ti_6Al_4V scaffolds with different diameters of dense cores (PT, PT-1.2, PT-1.8, PT-2.4), with porosity ranging from 50% to 75% and pore diameters of approximately 400 μm. Mechanical testing revealed that PT-1.8 exhibited optimal performance, with an elastic modulus (22.95 GPa) matching that of mandibular bone, along with a yield strength (330.91 MPa) and effective fatigue strength (165.46 MPa). This design ensures that the inner dense structure meets mechanical demands while the outer porous structure facilitates bone ingrowth, significantly enhancing mechanical properties without substantially sacrificing porosity.

However, beyond mechanical performance, surface biocompatibility is critical for rapid osseointegration

between implants and surrounding bone tissue. Iezzi *et al.*[198] performed organic acid etching on Ti_6Al_4V porous implants fabricated by LPBF. After acid etching, due to the high micro-nano roughness, the proliferation of osteoblasts increased by 38.76%, and calcium deposition increased by 42.75%. Meanwhile, the porous structure provided a three-dimensional growth space for cells, significantly enhancing the potential for osseointegration. Qin *et al.*[64] further optimized surface modification strategies for Ti implants by applying sandblasting, acid etching, and alkali etching to LPBF-fabricated implants with 30% porosity, as shown in Figure 13B. The surface roughness of the material reached the ideal value of 4.58 μm. The hydrophilicity, osteoblast activity and mineralization ability were significantly improved, while sufficient compressive strength was maintained. Compared to dense implants, the porous structure promotes nutrient transport and bone ingrowth, while composite surface modification further

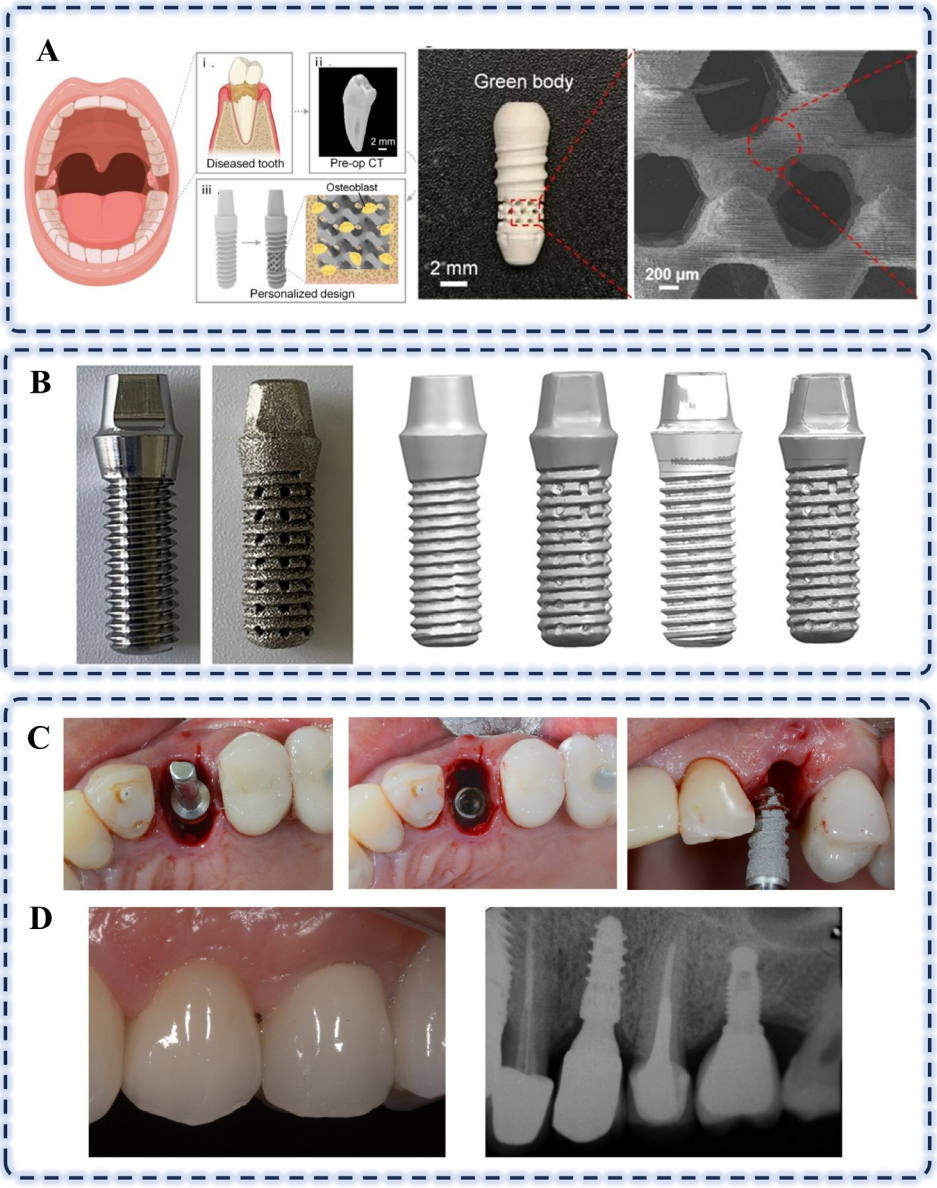

Figure 13. The application of titanium implants in dentistry. (A) The design and manufacture of piezoelectric dental implants. Reprinted with permission from Chen *et al.*[196] Copyright © 2026 Nature. (B) Traditional machine tool processing and additive manufacturing of dental implants. Reprinted with permission from Qin *et al.*[64] Copyright © 2023 Frontiers. (C) The implantation process of Ti alloy dental implant. (D) CT images of bone integration of AM Ti alloy after three years. Reprinted with permission from Tunchel *et al.*[199] Copyright © 2016, Wiley.

enhances bioactivity, achieving a synergistic improvement in mechanical performance and biocompatibility. Chen *et al.*[196] fabricated an occlusal-driven autonomous piezoelectric dental implant, as shown in Figure 13A. Using BCZT ($Ba_{0.85}Ca_{0.15}Zr_{0.1}Ti_{0.9}O_3$) powder with a high piezoelectric coefficient, they produced a TPMS bionic porous structure via vat photopolymerization 3D printing. The porosity was adjustable within the range of 0.3–0.7, while the compressive strength reached 16.6–87.2 MPa, and the elastic modulus closely matched that of human cancellous bone. Under physiological occlusal pressure, the implant stably generated electrical signals, which induced piezoelectric catalysis to produce reactive oxygen species. This resulted in bactericidal rates of 75.9% against *S. aureus* and 99.8% against *Porphyromonas gingivalis*. Additionally, it promoted macrophage polarization toward the anti-inflammatory M2 phenotype, significantly alleviating inflammatory responses.

In clinical validation, Tunchel *et al.*[199] used SLS to fabricate porous Ti_6Al_4V implants (surface roughness Ra = 66.8 μm) and conducted a 3-year follow-up study involving 82 patients with 110 implants (65 maxillary, 45 mandibular), as shown in Figure 13C and 13D. The implant survival rate within 3 years was 94.5%, and the marginal bone resorption at 1 year and 3 years was 0.75 mm ± 0.32 and 0.89 mm ± 0.45, respectively, both within clinically acceptable ranges. This process enables precise control the pore distribution and surface morphology, promoting bone ingrowth and mechanical interlocking, thereby demonstrating the reliability of AM Ti alloy implants in single-tooth replacement.

In summary, AM Ti alloy dental implants address challenges such as morphological mismatch, dimensional incompatibility, and slow osseointegration through personalized customization and multilevel surface modification techniques. In the future, large-scale clinical trials will be necessary to confirm the reliability and safety of porous dental implants.

5. Summary and prospects

This article provides a comprehensive exploration of the widespread applications of AM Ti alloys in the field of biomedical implants, systematically introducing structural design, surface modification technology, as well as clinical applications. The main conclusions are as follows:

(i) Porous structure design is a core strategy for enhancing the biological and mechanical compatibility of implants, where porosity, pore size, and pore morphology directly influence performance. Computer-aided technologies such as FEA and ML have supported the optimization of pore parameters and mechanical properties. For the repair of bone defects, the appropriate porosity range of bone implants prepared by LPBF is 60–70%, and the suitable pore size range is 500–700 μm. The appropriate porosity range of bone implants prepared by EBPBF is 70–75%, and the pore size range is 800–1,000 μm. The pore structure of these parameters can achieve mechanical compatibility with human bones, thereby reducing the stress shielding effect. TPMS structures outperform traditional lattice structures in terms of mechanical isotropy and biocompatibility. Furthermore, the gradient biomimetic structure design mimics the hierarchical structure of natural bone tissue, demonstrating a strong ability for bone integration.

(ii) Surface modification techniques address the shortcomings of insufficient surface activity and high roughness of AM Ti alloys. Mechanical, physical, chemical, and electrochemical modification techniques enhance bone integration efficiency, antibacterial performance, and corrosion resistance by constructing bioactive coatings, introducing antibacterial elements, or regulating topological structures. Multifunctional composite surface modification technology, by constructing multi-layer coatings on the surface of titanium scaffolds, enables them to possess multi-source stimulus responsiveness and controllable drug release functions, demonstrating significant potential in the field of bone implant modification.

(iii) AM Ti alloy implants have been successfully applied in joint replacements, spinal fusion, pelvic reconstruction, and dental implants. Personalized customization enables precise anatomical matching with patients, reducing surgical trauma. Clinical validation demonstrates that AM Ti alloys exhibit superior repair outcomes and reliability compared to traditional implants in scenarios such as complex bone defect repair and dental implant replacements.

In the future, the development of AM Ti alloy implants will focus on adaptability and functionalization. In terms of adaptability, further integration of medical imaging, numerical simulation, and topology optimization technologies is needed to achieve precise matching between implant pore structures and individual bone tissue characteristics. In terms of surface functionalization, it is necessary to consider designing multifunctional coatings that include natural biomimicry, strong interfacial stability, intelligent responsiveness, and controlled drug release to address complex clinical issues such as bone infections. Additionally, it is necessary to enhance the standardization and efficiency of the AM process, and conduct longer-term clinical follow-up studies to improve the long-term

safety and effectiveness data of the implants. With the deep integration of materials science, manufacturing technology, and medicine, AM Ti alloy implants have the potential to reshape the landscape of orthopedic medical devices.

Acknowledgments

None.

Funding

The authors acknowledge the National Key Research and Development Program of China (Grant Nos. 2024YFE0109000), the National Natural Science Foundation of China (Grant Nos. 52274387, 52311530772), the Fundamental Research Funds for the Central Universities (project number YG2024LC04), and the Fundamental Research Funds for the Central Universities (YG2023QNA21).

Conflict of interest

Liqiang Wang is an Editorial Board Member of this journal and Guest Editor of this special issue, but was not in any way involved in the editorial and peer-review process conducted for this paper, directly or indirectly. The authors declare that they have no known competing financial interests or personal relationships that could have appeared to influence the work reported in this paper.

Author contributions

Conceptualization: Shunyu Yao, Fengcang Ma, Liqiang Wang, Yanhua Chen, Vladimir Vasilievich Uglov
Visualization: Shunyu Yao, Fengcang Ma, Liqiang Wang
Writing–original draft: Shunyu Yao, Deyu Jiang
Writing–review & editing: All authors

Ethics approval and consent to participate

Not applicable.

Consent for publication

Not applicable.

Availability of data

Not applicable.

References

1. Briggs AM, Cross MJ, Hoy DG, *et al*. Musculoskeletal Health Conditions Represent a Global Threat to Healthy Aging: A Report for the 2015 World Health Organization World Report on Ageing and Health. *Gerontologist*. 2016;56(Suppl 2):S243-S255.

   doi: 10.1093/geront/gnw002

2. Westrick ER, Bernstein M, Little MT, Marecek GS, Scolaro JA. Orthopaedic Advances: Use of Three-Dimensional Metallic Implants for Reconstruction of Critical Bone Defects After Trauma. *J Am Acad Orthop Surg*. 2023;31(18):e685-e693.

   doi: 10.5435/JAAOS-D-22-00676

3. Meng M, Wang J, Huang H, Liu X, Zhang J, Li Z. 3D printing metal implants in orthopedic surgery: Methods, applications and future prospects. *J Orthop Transl*. 2023;42:94-112.

   doi: 10.1016/j.jot.2023.08.004

4. Zhao L, Pei X, Jiang L, *et al*. Bionic design and 3D printing of porous titanium alloy scaffolds for bone tissue repair. *Compos Part B Eng*. 2019;162:154-161.

   doi: 10.1016/j.compositesb.2018.10.094

5. Cordeiro JM, Beline T, Ribeiro ALR, *et al*. Development of binary and ternary titanium alloys for dental implants. *Dent Mater*. 2017;33(11):1244-1257.

   doi: 10.1016/j.dental.2017.07.013

6. Li Y, Jiang D, Zhu R, Yang C, Wang L, Zhang LC. Revolutionizing medical implant fabrication: advances in additive manufacturing of biomedical metals. *Int J Extrem Manuf*. 2025;7(2):022002.

   doi: 10.1088/2631-7990/ad92cc

7. Abd-Elaziem W, Darwish MA, Hamada A, Daoush WM. Titanium-Based alloys and composites for orthopedic implants Applications: A comprehensive review. *Mater Des*. 2024;241:112850.

   doi: 10.1016/j.matdes.2024.112850

8. Guo AXY, Cheng L, Zhan S, *et al*. Biomedical applications of the powder-based 3D printed titanium alloys: A review. *J Mater Sci Technol*. 2022;125:252-264.

   doi: 10.1016/j.jmst.2021.11.084

9. Cui YW, Wang L, Zhang LC. Towards load-bearing biomedical titanium-based alloys: From essential requirements to future developments. *Prog Mater Sci*. 2024;144:101277.

   doi: 10.1016/j.pmatsci.2024.101277

10. Sun XD, Liu TT, Wang QQ, Zhang J, Cao MS. Surface Modification and Functionalities for Titanium Dental Implants. *ACS Biomater Sci Eng*. 2023;9(8):4442-4461.

    doi: 10.1021/acsbiomaterials.3c00183

11. Mao C, Yu W, Jin M, *et al*. Mechanobiologically optimized Ti–35Nb–2Ta–3Zr improves load transduction and enhances bone remodeling in tilted dental implant therapy. *Bioact Mater*. 2022;16:15-26.

    doi: 10.1016/j.bioactmat.2022.03.005

12. Shao L, Du Y, Dai K, *et al*. β-Ti Alloys for Orthopedic and Dental Applications: A Review of Progress on Improvement

of Properties through Surface Modification. *Coatings*. 2021;11(12):1446.

doi: 10.3390/coatings11121446

13. Zhang E, Zhao X, Hu J, Wang R, Fu S, Qin G. Antibacterial metals and alloys for potential biomedical implants. *Bioact Mater*. 2021;6(8):2569-2612.

doi: 10.1016/j.bioactmat.2021.01.030

14. Sidhu SS, Singh H, Gepreel MAH. A review on alloy design, biological response, and strengthening of β-titanium alloys as biomaterials. *Mater Sci Eng C*. 2021;121:111661.

doi: 10.1016/j.msec.2020.111661

15. Xu Z, Zhang Y, Wu Y, *et al*. In Vitro and In Vivo Analysis of the Effects of 3D-Printed Porous Titanium Alloy Scaffold Structure on Osteogenic Activity. *Biomed Res Int*. 2022;2022(1):8494431.

doi: 10.1155/2022/8494431

16. Wang Z, Zhang M, Liu Z, *et al*. Biomimetic design strategy of complex porous structure based on 3D printing Ti-6Al-4V scaffolds for enhanced osseointegration. *Mater Des*. 2022;218:110721.

doi: 10.1016/j.matdes.2022.110721

17. Song C, Liu L, Deng Z, *et al*. Research progress on the design and performance of porous titanium alloy bone implants. *J Mater Res Technol*. 2023;23:2626-2641.

doi: 10.1016/j.jmrt.2023.01.155

18. Qu Z, Zhang Z, Liu R, *et al*. High fatigue resistance in a titanium alloy via near-void-free 3D printing. *Nature*. 2024;626(8001):999-1004.

doi: 10.1038/s41586-024-07048-1

19. Zhang J, Bermingham MJ, Otte J, *et al*. Ultrauniform, strong, and ductile 3D-printed titanium alloy through bifunctional alloy design. *Science*. 2024;383(6683):639-645.

doi: 10.1126/science.adj0141

20. Tang Z, Yu D, Bao S, *et al*. Porous Titanium Scaffolds with Mechanoelectrical Conversion and Photothermal Function: A Win-Win Strategy for Bone Reconstruction of Tumor-Resected Defects. *Adv Healthc Mater*. 2024;13(7):2302901.

doi: 10.1002/adhm.202302901

21. Kaseem M, Fatimah S, Nashrah N, Ko YG. Recent progress in surface modification of metals coated by plasma electrolytic oxidation: Principle, structure, and performance. *Prog Mater Sci*. 2021;117:100735.

doi: 10.1016/j.pmatsci.2020.100735

22. Li G, Ma F, Liu P, *et al*. Review of micro-arc oxidation of titanium alloys: Mechanism, properties and applications. *J Alloys Compd*. 2023;948:169773.

doi: 10.1016/j.jallcom.2023.169773

23. Han X, Ma J, Tian A, *et al*. Surface modification techniques of titanium and titanium alloys for biomedical orthopaedics applications: A review. *Colloids Surf B Biointerfaces*. 2023;227:113339.

doi: 10.1016/j.colsurfb.2023.113339

24. Yao Y, Yi Z, Chong WJ, *et al*. Micro-arc oxidation surface-modification of titanium alloys for biomedical applications: Mechanisms, advances, challenges, and prospects. *Prog Mater Sci*. 2026;159:101654.

doi: 10.1016/j.pmatsci.2026.101654

25. Luo X, Yang C, Li D, Zhang LC. Laser Powder Bed Fusion of Beta-Type Titanium Alloys for Biomedical Application: A Review. *Acta Metall Sin (Engl Lett)*. 2024;37(1):17-28.

doi: 10.1007/s40195-023-01654-0

26. Armstrong M, Mehrabi H, Naveed N. An overview of modern metal additive manufacturing technology. *J Manuf Process*. 2022;84:1001-1029.

doi: 10.1016/j.jmapro.2022.10.060

27. Chattopadhyay S, Mahapatra SD, Mandal NK. Advancements and challenges in additive manufacturing: a comprehensive review. *Eng Res Express*. 2024;6(1):012505.

doi: 10.1088/2631-8695/ad30b1

28. Sing SL, Huang S, Goh GD, *et al*. Emerging metallic systems for additive manufacturing: In-situ alloying and multi-metal processing in laser powder bed fusion. *Prog Mater Sci*. 2021;119:100795.

doi: 10.1016/j.pmatsci.2021.100795

29. Haase F, Siemers C, Rösler J. Laser powder bed fusion (LPBF) of commercially pure titanium and alloy development for the LPBF process. *Front Bioeng Biotechnol*. 2023;11:1260925.

doi: 10.3389/fbioe.2023.1260925

30. Behjat A, Sanaei S, Mosallanejad MH, *et al*. A novel titanium alloy for load-bearing biomedical implants: Evaluating the antibacterial and biocompatibility of Ti536 produced via electron beam powder bed fusion additive manufacturing process. *Biomater Adv*. 2024;163:213928.

doi: 10.1016/j.bioadv.2024.213928

31. Ibrahim P, Garrard R, Attallah MM. Laser powder bed fusion of a β titanium alloy: Microstructural development, post-processing, and mechanical behaviour. *Mater Sci Eng A*. 2024;905:146617.

doi: 10.1016/j.msea.2024.146617

32. Thijs L, Verhaeghe F, Craeghs T, Humbeeck JV, Kruth JP. A study of the microstructural evolution during selective laser melting of Ti–6Al–4V. *Acta Mater*. 2010;58(9):3303-3312.

doi: 10.1016/j.actamat.2010.02.004

33. Li G, Zhou X, Zhang J, Yuan M, Chen Z. Effects of electron beam current on local microstructure characteristics and

tensile behaviors of Ti–6Al–4V alloys fabricated by electron beam melting. *Mater Sci Eng A*. 2024;912:146966.

doi: 10.1016/j.msea.2024.146966

34. He S, Xiao F, Li L, *et al*. Design biomedical β-Ti alloys with exceptional strength-ductility balance via domain knowledge-based machine learning. *Acta Mater*. 2025;301:121550.

doi: 10.1016/j.actamat.2025.121550

35. Xiao F, Ye J hui, Huang C xiao, *et al*. Gradient gyroid Ti6Al4V scaffolds with TiO2 surface modification: Promising approach for large bone defect repair. *Biomater Adv*. 2024;161:213899.

doi: 10.1016/j.bioadv.2024.213899

36. Taghian M, Pilehvar Meibody A, Saboori A, Iuliano L. Toward closed-loop quality assurance in powder bed fusion additive manufacturing: Defect detection, machine learning, and computational modeling. *J Manuf Process*. 2026;160:50-81.

doi: 10.1016/j.jmapro.2026.01.026

37. Aufa AN, Hassan MZ, Ismail Z. Recent advances in Ti-6Al-4V additively manufactured by selective laser melting for biomedical implants: Prospect development. *J Alloys Compd*. 2022;896:163072.

doi: 10.1016/j.jallcom.2021.163072

38. Liu J, Zhang K, Bermingham MJ, *et al*. Fatigue and damage tolerance performance of additively-manufactured titanium alloys for structural application: A comprehensive review. *Mater Sci Eng R Rep*. 2026;167:101135.

doi: 10.1016/j.mser.2025.101135

39. Li G, Liu W, Liang L, Liu T, Tian Y, Wu H. Preparing Sr-containing nano-structures on micro-structured titanium alloy surface fabricated by additively manufacturing to enhance the anti-inflammation and osteogenesis. *Colloids Surf B Biointerfaces*. 2022;218:112762.

doi: 10.1016/j.colsurfb.2022.112762

40. Civantos A, Martínez-Campos E, Ramos V, Elvira C, Gallardo A, Abarrategi A. Titanium Coatings and Surface Modifications: Toward Clinically Useful Bioactive Implants. *ACS Biomater Sci Eng*. 2017;3(7):1245-1261.

doi: 10.1021/acsbiomaterials.6b00604

41. Xie X, Chang L, Chen B, Li J, Huang H, Guo Z. Promote the catalytic performance and service life of Ti-based oxide coatings through sandblasting. *Ionics*. 2022;28(5):2501-2511.

doi: 10.1007/s11581-021-04408-z

42. Chen R, Xu J, Zhao F, Wu Y, Zhang J. Preparation of Microstructure Laser Ablation and Multiple Acid-Etching Composites on the Surfaces of Medical Titanium Alloy TC4 by Laser Ablation and Multiple Acid-Etching, and Study of Frictional Properties of the Processed Surfaces. *Metals*. 2022;12(7):1148.

doi: 10.3390/met12071148

43. Liu X, Niu Y, Xie W, Wei D, Du Q. Comparative investigations of in vitro and in vivo bioactivity of titanium vs. Ti–24Nb–4Zr–8Sn alloy before and after sandblasting and acid etching. *RSC Adv*. 2020;10(40):23582-23591.

doi: 10.1039/D0RA00280A

44. Rautray TR, Narayanan R, Kim KH. Ion implantation of titanium based biomaterials. *Prog Mater Sci*. 2011;56(8):1137-1177.

doi: 10.1016/j.pmatsci.2011.03.002

45. Lenis JA, Bejarano G, Rico P, Ribelles JLG, Bolívar FJ. Development of multilayer Hydroxyapatite - Ag/TiN-Ti coatings deposited by radio frequency magnetron sputtering with potential application in the biomedical field. *Surf Coat Technol*. 2019;377:124856.

doi: 10.1016/j.surfcoat.2019.06.097

46. Su Y, Komasa S, Sekino T, Nishizaki H, Okazaki J. Nanostructured Ti6Al4V alloy fabricated using modified alkali-heat treatment: Characterization and cell adhesion. *Mater Sci Eng C*. 2016;59:617-623.

doi: 10.1016/j.msec.2015.10.077

47. Tsukimura N, Ueno T, Iwasa F, *et al*. Bone integration capability of alkali- and heat-treated nanobimorphic Ti–15Mo–5Zr–3Al. *Acta Biomater*. 2011;7(12):4267-4277.

doi: 10.1016/j.actbio.2011.08.016

48. Dai X, Zhao J, Qi S, *et al*. Enhanced biological performance of Sr2+-doped nanorods on titanium implants by surface thermal-chemical treatment. *J Mater Sci Mater Med*. 2025;36(1):54.

doi: 10.1007/s10856-025-06898-z

49. Advincula MC, Rahemtulla FG, Advincula RC, Ada ET, Lemons JE, Bellis SL. Osteoblast adhesion and matrix mineralization on sol–gel-derived titanium oxide. *Biomaterials*. 2006;27(10):2201-2212.

doi: 10.1016/j.biomaterials.2005.11.014

50. Bai W, Ma F, Zhao J, *et al*. Preparation of a composite coating of bimodal TiO2 nanotubes with deposited Ag nanoparticles and its biological performance. *Mater Chem Phys*. 2025;339:130710.

doi: 10.1016/j.matchemphys.2025.130710

51. Gulati K, Zhang Y, Di P, Liu Y, Ivanovski S. Research to Clinics : Clinical Translation Considerations for Anodized Nano-Engineered Titanium Implants. *ACS Biomater Sci Eng*. 2022;8(10):4077-4091.

doi: 10.1021/acsbiomaterials.1c00529

52. Liu L, Ma F, Liu P, *et al*. Preparation and antibacterial

properties of ZnSr-doped micro-arc oxidation coatings on titanium. *Surf Coat Technol*. 2023;462:129469.

doi: 10.1016/j.surfcoat.2023.129469

53. Qi S, Kang B, Yao C, *et al*. Cerium doped TiO2 coating with superior antibacterial property and biocompatibility prepared by micro-arc oxidation. *Mater Des*. 2023;234:112312.

doi: 10.1016/j.matdes.2023.112312

54. Shojaei AR, Soleimany Zefreh A, Malekli M, Ramezanzadeh B, Eivaz Mohammadloo H. Sustainable metal-organic framework (MOF) bio-films for biomedical applications. *Sustain Mater Technol*. 2025;46:e01633.

doi: 10.1016/j.susmat.2025.e01633

55. Sun M, Wang J, Huang X, *et al*. Ultrasound-driven radical chain reaction and immunoregulation of piezoelectric-based hybrid coating for treating implant infection. *Biomaterials*. 2024;307:122532.

doi: 10.1016/j.biomaterials.2024.122532

56. Blakey-Milner B, Gradl P, Snedden G, *et al*. Metal additive manufacturing in aerospace: A review. *Mater Des*. 2021;209:110008.

doi: 10.1016/j.matdes.2021.110008

57. Depboylu FN, Yasa E, Poyraz Ö, Minguella-Canela J, Korkusuz F, De Los Santos López MA. Titanium based bone implants production using laser powder bed fusion technology. *J Mater Res Technol*. 2022;17:1408-1426.

doi: 10.1016/j.jmrt.2022.01.087

58. Chen H, Han Q, Wang C, Liu Y, Chen B, Wang J. Porous Scaffold Design for Additive Manufacturing in Orthopedics: A Review. *Front Bioeng Biotechnol*. 2020;8:609.

doi: 10.3389/fbioe.2020.00609

59. Vaiani L, Boccaccio A, Uva AE, *et al*. Ceramic Materials for Biomedical Applications: An Overview on Properties and Fabrication Processes. *J Funct Biomater*. 2023;14(3):146.

doi: 10.3390/jfb14030146

60. Al-Ketan O, Abu Al-Rub RK. Multifunctional Mechanical Metamaterials Based on Triply Periodic Minimal Surface Lattices. *Adv Eng Mater*. 2019;21(10):1900524.

doi: 10.1002/adem.201900524

61. Gawronska E, Dyja R. A Numerical Study of Geometry's Impact on the Thermal and Mechanical Properties of Periodic Surface Structures. *Materials*. 2021;14(2):427.

doi: 10.3390/ma14020427

62. Liu W, Zhang Y, Lyu Y, Bosiakov S, Liu Y. Inverse design of anisotropic bone scaffold based on machine learning and regenerative genetic algorithm. *Front Bioeng Biotechnol*. 2023;11:1241151.

doi: 10.3389/fbioe.2023.1241151

63. Sun C, Shang G. Application and Development of 3D Printing in Medical Field. *Mod Mech Eng*. 2020;10(3):25-33.

doi: 10.4236/mme.2020.103003

64. Qin Z, He Y, Gao J, *et al*. Surface modification improving the biological activity and osteogenic ability of 3D printing porous dental implants. *Front Mater*. 2023;10:1183902.

doi: 10.3389/fmats.2023.1183902

65. Ahmadi S, Yavari S, Wauthle R, *et al*. Additively Manufactured Open-Cell Porous Biomaterials Made from Six Different Space-Filling Unit Cells: The Mechanical and Morphological Properties. *Materials*. 2015;8(4):1871-1896.

doi: 10.3390/ma8041871

66. Li Y, Jiang D, Zhao R, Wang X, Wang L, Zhang LC. High Mechanical Performance of Lattice Structures Fabricated by Additive Manufacturing. *Metals*. 2024;14(10):1165.

doi: 10.3390/met14101165

67. Al-Ketan O, Rowshan R, Abu Al-Rub RK. Topology-mechanical property relationship of 3D printed strut, skeletal, and sheet based periodic metallic cellular materials. *Addit Manuf*. 2018;19:167-183.

doi: 10.1016/j.addma.2017.12.006

68. Zhang Y, Wei D, Chen Y, *et al*. Non-negligible role of gradient porous structure in superelasticity deterioration and improvement of NiTi shape memory alloys. *J Mater Sci Technol*. 2024;186:48-63.

doi: 10.1016/j.jmst.2023.10.053

69. Lv Y, Wang B, Liu G, *et al*. Design of bone-like continuous gradient porous scaffold based on triply periodic minimal surfaces. *J Mater Res Technol*. 2022;21:3650-3665.

doi: 10.1016/j.jmrt.2022.10.160

70. Arabnejad S, Burnett Johnston R, Pura JA, Singh B, Tanzer M, Pasini D. High-strength porous biomaterials for bone replacement: A strategy to assess the interplay between cell morphology, mechanical properties, bone ingrowth and manufacturing constraints. *Acta Biomater*. 2016;30:345-356.

doi: 10.1016/j.actbio.2015.10.048

71. Lei H, Zhou Z, Liu J, *et al*. Structural Optimization of 3D-Printed Porous Titanium Implants Promotes Bone Regeneration for Enhanced Biological Fixation. *ACS Appl Mater Interfaces*. 2025;17(12):18059-18073.

doi: 10.1021/acsami.4c22401

72. Parisien A, ElSayed MSA, Frei H. Mechanoregulation modelling of stretching versus bending dominated periodic cellular solids. *Mater Today Commun*. 2022;33:104315.

doi: 10.1016/j.mtcomm.2022.104315

73. Ali D, Ozalp M, Blanquer SBG, Onel S. Permeability and fluid flow-induced wall shear stress in bone scaffolds with TPMS and lattice architectures: A CFD analysis. *Eur J Mech*

B Fluids. 2020;79:376-385.

doi: 10.1016/j.euromechflu.2019.09.015

74. Wang B, Zhou C, Zhou J, *et al*. Niti minimal surface porous scaffolds matching human bone characteristics: mechanical, permeability and osteogenic properties. *Virtual Phys Prototyp*. 2026;21(1):e2633475.

doi: 10.1080/17452759.2026.2633475

75. Werner M, Blanquer SBG, Haimi SP, *et al*. Surface Curvature Differentially Regulates Stem Cell Migration and Differentiation via Altered Attachment Morphology and Nuclear Deformation. *Adv Sci*. 2017;4(2):1600347.

doi: 10.1002/advs.201600347

76. Ataee A, Li Y, Fraser D, Song G, Wen C. Anisotropic Ti-6Al-4V gyroid scaffolds manufactured by electron beam melting (EBM) for bone implant applications. *Mater Des*. 2018;137:345-354.

doi: 10.1016/j.matdes.2017.10.040

77. Santos J, Pires T, Gouveia BP, Castro APG, Fernandes PR. On the permeability of TPMS scaffolds. *J Mech Behav Biomed Mater*. 2020;110:103932.

doi: 10.1016/j.jmbbm.2020.103932

78. Bobbert FSL, Lietaert K, Eftekhari AA, *et al*. Additively manufactured metallic porous biomaterials based on minimal surfaces: A unique combination of topological, mechanical, and mass transport properties. *Acta Biomater*. 2017;53:572-584.

doi: 10.1016/j.actbio.2017.02.024

79. Deng F, Liu L, Li Z, Liu J. 3D printed Ti6Al4V bone scaffolds with different pore structure effects on bone ingrowth. *J Biol Eng*. 2021;15(1):4.

doi: 10.1186/s13036-021-00255-8

80. Gandhi R, Salmi M, Roy B, Pagliari L, Concli F. Mechanical performance, fatigue behaviour, and biointegration of additively manufactured architected lattices. *Virtual Phys Prototyp*. 2025;20(1):e2530733.

doi: 10.1080/17452759.2025.2530733

81. Lv Y, Wang B, Liu G, *et al*. Metal Material, Properties and Design Methods of Porous Biomedical Scaffolds for Additive Manufacturing: A Review. *Front Bioeng Biotechnol*. 2021;9:641130.

doi: 10.3389/fbioe.2021.641130

82. Kapat K, Srivas PK, Rameshbabu AP, *et al*. Influence of Porosity and Pore-Size Distribution in Ti6 Al4 V Foam on Physicomechanical Properties, Osteogenesis, and Quantitative Validation of Bone Ingrowth by Micro-Computed Tomography. *ACS Appl Mater Interfaces*. 2017;9(45):39235-39248.

doi: 10.1021/acsami.7b13960

83. Taniguchi N, Fujibayashi S, Takemoto M, *et al*. Effect of pore size on bone ingrowth into porous titanium implants fabricated by additive manufacturing: An in vivo experiment. *Mater Sci Eng C*. 2016;59:690-701.

doi: 10.1016/j.msec.2015.10.069

84. Liang H, Yang Y, Xie D, *et al*. Trabecular-like Ti-6Al-4V scaffolds for orthopedic: fabrication by selective laser melting and in vitro biocompatibility. *J Mater Sci Technol*. 2019;35(7):1284-1297.

doi: 10.1016/j.jmst.2019.01.012

85. Chen Z, Yan X, Yin S, *et al*. Influence of the pore size and porosity of selective laser melted Ti6Al4V ELI porous scaffold on cell proliferation, osteogenesis and bone ingrowth. *Mater Sci Eng C*. 2020;106:110289.

doi: 10.1016/j.msec.2019.110289

86. Yan X, Li Q, Yin S, *et al*. Mechanical and in vitro study of an isotropic Ti6Al4V lattice structure fabricated using selective laser melting. *J Alloys Compd*. 2019;782:209-223.

doi: 10.1016/j.jallcom.2018.12.220

87. Zhang Y, Sun N, Zhu M, *et al*. The contribution of pore size and porosity of 3D printed porous titanium scaffolds to osteogenesis. *Biomater Adv*. 2022;133:112651.

doi: 10.1016/j.msec.2022.112651

88. Ouyang P, Dong H, He X, *et al*. Hydromechanical mechanism behind the effect of pore size of porous titanium scaffolds on osteoblast response and bone ingrowth. *Mater Des*. 2019;183:108151.

doi: 10.1016/j.matdes.2019.108151

89. Kelly CN, Evans NT, Irvin CW, Chapman SC, Gall K, Safranski DL. The effect of surface topography and porosity on the tensile fatigue of 3D printed Ti-6Al-4V fabricated by selective laser melting. *Mater Sci Eng C*. 2019;98:726-736.

doi: 10.1016/j.msec.2019.01.024

90. Pobloth AM, Checa S, Razi H, *et al*. Mechanobiologically optimized 3D titanium-mesh scaffolds enhance bone regeneration in critical segmental defects in sheep. *Sci Transl Med*. 2018;10(423):eaam8828.

doi: 10.1126/scitranslmed.aam8828

91. Li G, Wang L, Pan W, *et al*. In vitro and in vivo study of additive manufactured porous Ti6Al4V scaffolds for repairing bone defects. *Sci Rep*. 2016;6(1):34072.

doi: 10.1038/srep34072

92. Goto M, Matsumine A, Yamaguchi S, *et al*. Osteoconductivity of bioactive Ti-6Al-4V implants with lattice-shaped interconnected large pores fabricated by electron beam melting. *J Biomater Appl*. 2021;35(9):1153-1167.

doi: 10.1177/0885328220968218

93. Zhang C, Zhang L, Liu L, *et al*. Mechanical behavior of a

titanium alloy scaffold mimicking trabecular structure. *J Orthop Surg Res*. 2020;15(1):40.

doi: 10.1186/s13018-019-1489-y

94. Hara D, Nakashima Y, Sato T, *et al*. Bone bonding strength of diamond-structured porous titanium-alloy implants manufactured using the electron beam-melting technique. *Mater Sci Eng C*. 2016;59:1047-1052.

doi: 10.1016/j.msec.2015.11.025

95. Wang C, Xu D, Li S, *et al*. Effect of Pore Size on the Physicochemical Properties and Osteogenesis of Ti6Al4V Porous Scaffolds with Bionic Structure. *ACS Omega*. 2020;5(44):28684-28692.

doi: 10.1021/acsomega.0c03824

96. Arabnejad S, Johnston B, Tanzer M, Pasini D. Fully porous 3D printed titanium femoral stem to reduce stress-shielding following total hip arthroplasty. *J Orthop Res*. 2017;35(8):1774-1783.

doi: 10.1002/jor.23445

97. Yao B, Zhang Z, Li Z, *et al*. Compressive properties and energy absorption of selective laser melting formed Ti-6Al-4V porous radial gradient scaffold. *Powder Technol*. 2024;442:119856.

doi: 10.1016/j.powtec.2024.119856

98. Jia Y, Liu K, Zhang XS. Modulate stress distribution with bio-inspired irregular architected materials towards optimal tissue support. *Nat Commun*. 2024;15(1):4072.

doi: 10.1038/s41467-024-47831-2

99. Zhang L, Wang B, Song B, *et al*. 3D Printed Biomimetic Metamaterials with Graded Porosity and Tapering Topology for Improved Cell Seeding and Bone Regeneration. *Bioact Mater*. 2023;25:677-688.

doi: 10.1016/j.bioactmat.2022.07.009

100. Ye X, Shi X, Miao X, Lu P, Wu M. The influence mechanism of fractal design method on mechanical properties and corrosion behavior of sheet Gyroid porous structures formed by LPBF. *Mater Today Commun*. 2024;41:110373.

doi: 10.1016/j.mtcomm.2024.110373

101. Zhang J, Chen X, Sun Y, *et al*. Design of a biomimetic graded TPMS scaffold with quantitatively adjustable pore size. *Mater Des*. 2022;218:110665.

doi: 10.1016/j.matdes.2022.110665

102. Naqvi SMR, Gu J, Liu S, *et al*. Laser powder bed fusion additive manufacturing of Ti-6Al-4V dental implants with gradient porosity: Design, simulation, and biomechanical performance. *J Mater Sci*. 2026;61(1):594-616.

doi: 10.1007/s10853-025-11880-9

103. Zhang L, Li F, Yang Y, *et al*. Structure design of porous TC4 alloy with excellent mechanical properties prepared by laser-powder bed fusion. *Vacuum*. 2024;220:112818.

doi: 10.1016/j.vacuum.2023.112818

104. He X, Li Y, Bi Y, *et al*. Finite element analysis of temperature and residual stress profiles of porous cubic Ti-6Al-4V titanium alloy by electron beam melting. *J Mater Sci Technol*. 2020;44:191-200.

doi: 10.1016/j.jmst.2020.01.033

105. Sarkar D, Kapil A, Sharma A. Advances in computational modeling for laser powder bed fusion additive manufacturing: A comprehensive review of finite element techniques and strategies. *Addit Manuf*. 2024;85:104157.

doi: 10.1016/j.addma.2024.104157

106. Wang L, Huang H, Yuan H, *et al*. In vitro fatigue behavior and in vivo osseointegration of the auxetic porous bone screw. *Acta Biomater*. 2023;170:185-201.

doi: 10.1016/j.actbio.2023.08.040

107. Yu G, Li Z, Li S, *et al*. The select of internal architecture for porous Ti alloy scaffold: A compromise between mechanical properties and permeability. *Mater Des*. 2020;192:108754.

doi: 10.1016/j.matdes.2020.108754

108. Shum JM, Gadomski BC, Tredinnick SJ, *et al*. Enhanced bone formation in locally-optimised, low-stiffness additive manufactured titanium implants: An in silico and in vivo tibial advancement study. *Acta Biomater*. 2023;156:202-213.

doi: 10.1016/j.actbio.2022.04.006

109. Moussa A, Rahman S, Xu M, Tanzer M, Pasini D. Topology optimization of 3D-printed structurally porous cage for acetabular reinforcement in total hip arthroplasty. *J Mech Behav Biomed Mater*. 2020;105:103705.

doi: 10.1016/j.jmbbm.2020.103705

110. Srivastava P, Singh VP. FEM-based designing and modelling of a porous customised hip implant stem using n-Topology software. *Aust J Mech Eng*. 2026;24(1):118-126.

doi: 10.1080/14484846.2025.2506264

111. Peng W ming, Cheng K jie, Liu Y feng, *et al*. Biomechanical and Mechanostat analysis of a titanium layered porous implant for mandibular reconstruction: The effect of the topology optimization design. *Mater Sci Eng C*. 2021;124:112056.

doi: 10.1016/j.msec.2021.112056

112. Wu C, Xu Y, Fang J, Li Q. Machine Learning in Biomaterials, Biomechanics/Mechanobiology, and Biofabrication: State of the Art and Perspective. *Arch Comput Methods Eng*. 2024.

doi: 10.1007/s11831-024-10100-y

113. Mao Y, Jiang D, Vladimir U, Jing Z, Wang L. Machine learning-driven additive manufacturing of biomedical metals: A review of forward prediction, inverse optimization, and quality control. *Eng Sci Addit Manuf*. 2025;1(4):025440031.

doi: 10.36922/ESAM025440031

114. Jiang D, Luo M, Liu C, *et al*. 3D Printing parameter optimisation combined with heat treatment for achieving high density and enhanced performance in refractory high-entropy alloys. *Virtual Phys Prototyp*. 2025;20(1):e2524524.

doi: 10.1080/17452759.2025.2524524

115. Jha R, Dulikravich GS. Discovery of New Ti-Based Alloys Aimed at Avoiding/Minimizing Formation of α" and ω-Phase Using CALPHAD and Artificial Intelligence. *Metals*. 2020;11(1):15.

doi: 10.3390/met11010015

116. Suwardi A, Wang F, Xue K, *et al*. Machine Learning-Driven Biomaterials Evolution. *Adv Mater*. 2022;34(1):2102703.

doi: 10.1002/adma.202102703

117. Peng B, Wei Y, Qin Y, *et al*. Machine learning-enabled constrained multi-objective design of architected materials. *Nat Commun*. 2023;14(1):6630.

doi: 10.1038/s41467-023-42415-y

118. Hu B, Wang Z, Du C, *et al*. Multi-objective Bayesian optimization accelerated design of TPMS structures. *Int J Mech Sci*. 2023;244:108085.

doi: 10.1016/j.ijmecsci.2022.108085

119. Zhang J, Zhao J, Rong Q, Yu W, Li X, Misra RDK. Machine learning guided prediction of mechanical properties of TPMS structures based on finite element simulation for biomedical titanium. *Mater Technol*. 2021.

doi: 10.1080/10667857.2021.1999558

120. Sing SL, An J, Yeong WY, Wiria FE. Laser and electron-beam powder-bed additive manufacturing of metallic implants: A review on processes, materials and designs. *J Orthop Res*. 2016;34(3):369-385.

doi: 10.1002/jor.23075

121. Benedetti M, Torresani E, Leoni M, *et al*. The effect of post-sintering treatments on the fatigue and biological behavior of Ti-6Al-4V ELI parts made by selective laser melting. *J Mech Behav Biomed Mater*. 2017;71:295-306.

doi: 10.1016/j.jmbbm.2017.03.024

122. Zhang LC, Chen LY, Wang L. Surface Modification of Titanium and Titanium Alloys: Technologies, Developments, and Future Interests. *Adv Eng Mater*. 2020;22(5):1901258.

doi: 10.1002/adem.201901258

123. Bagehorn S, Wehr J, Maier HJ. Application of mechanical surface finishing processes for roughness reduction and fatigue improvement of additively manufactured Ti-6Al-4V parts. *Int J Fatigue*. 2017;102:135-142.

doi: 10.1016/j.ijfatigue.2017.05.008

124. Zhang X, Guan S, Qiu J, *et al*. Atomic Layer Deposition of Tantalum Oxide Films on 3D-Printed Ti6Al4V Scaffolds with Enhanced Osteogenic Property for Orthopedic Implants. *ACS Biomater Sci Eng*. 2023;9(7):4197-4207.

doi: 10.1021/acsbiomaterials.3c00217

125. Heimann RB. Plasma-Sprayed Hydroxylapatite Coatings as Biocompatible Intermediaries Between Inorganic Implant Surfaces and Living Tissue. *J Therm Spray Technol*. 2018;27(8):1212-1237.

doi: 10.1007/s11666-018-0737-8

126. Zhou L, You J, Wang Z, *et al*. 3D printing monetite-coated Ti-6Al-4V surface with osteoimmunomodulatory function to enhance osteogenesis. *Biomater Adv*. 2022;134:112562.

doi: 10.1016/j.msec.2021.112562

127. Huang H, Wu Z, Yang Z, *et al*. In vitro application of drug-loaded hydrogel combined with 3D-printed porous scaffolds. *Biomed Mater*. 2022;17(6):065019.

doi: 10.1088/1748-605X/ac9943

128. Chudinova EA, Surmeneva MA, Timin AS, *et al*. Adhesion, proliferation, and osteogenic differentiation of human mesenchymal stem cells on additively manufactured Ti6Al4V alloy scaffolds modified with calcium phosphate nanoparticles. *Colloids Surf B Biointerfaces*. 2019;176:130-139.

doi: 10.1016/j.colsurfb.2018.12.047

129. Yang G, Liu H, Li A, Liu T, Lu Q, He F. Antibacterial Structure Design of Porous Ti6Al4V by 3D Printing and Anodic Oxidation. *Materials*. 2023;16(15):5206.

doi: 10.3390/ma16155206

130. Guilherme AS, Henriques GEP, Zavanelli RA, Mesquita MF. Surface roughness and fatigue performance of commercially pure titanium and Ti-6Al-4V alloy after different polishing protocols. *J Prosthet Dent*. 2005;93(4):378-385.

doi: 10.1016/j.prosdent.2005.01.010

131. Kim J, Lee H, Jang TS, *et al*. Characterization of Titanium Surface Modification Strategies for Osseointegration Enhancement. *Metals*. 2021;11(4):618.

doi: 10.3390/met11040618

132. Wennerberg A, Albrektsson T. Effects of titanium surface topography on bone integration: a systematic review. *Clin Oral Implants Res*. 2009;20(s4):172-184.

doi: 10.1111/j.1600-0501.2009.01775.x

133. Pyka G, Burakowski A, Kerckhofs G, *et al*. Surface Modification of Ti6Al4V Open Porous Structures Produced by Additive Manufacturing. *Adv Eng Mater*. 2012;14(6):363-370.

doi: 10.1002/adem.201100344

134. Rupp F, Liang L, Geis-Gerstorfer J, Scheideler L, Hüttig F. Surface characteristics of dental implants: A review. *Dent Mater*. 2018;34(1):40-57.

doi: 10.1016/j.dental.2017.09.007

135. Gittens RA, Olivares-Navarrete R, Schwartz Z, Boyan BD. Implant osseointegration and the role of microroughness and nanostructures: Lessons for spine implants. *Acta Biomater*. 2014;10(8):3363-3371.

doi: 10.1016/j.actbio.2014.03.037

136. Buser D, Janner SFM, Wittneben J, Brägger U, Ramseier CA, Salvi GE. 10-Year Survival and Success Rates of 511 Titanium Implants with a Sandblasted and Acid-Etched Surface: A Retrospective Study in 303 Partially Edentulous Patients. *Clin Implant Dent Relat Res*. 2012;14(6):839-851.

doi: 10.1111/j.1708-8208.2012.00456.x

137. Zhang L, Chen L. A Review on Biomedical Titanium Alloys: Recent Progress and Prospect. *Adv Eng Mater*. 2019;21(4):1801215.

doi: 10.1002/adem.201801215

138. Huang HL, Tsai MT, Chang YY, Lin YJ, Hsu JT. Fabrication of a Novel Ta(Zn)O Thin Film on Titanium by Magnetron Sputtering and Plasma Electrolytic Oxidation for Cell Biocompatibilities and Antibacterial Applications. *Metals*. 2020;10(5):649.

doi: 10.3390/met10050649

139. Jörg F, Betül KA, Heiner M, Gerhard K, Erwin BR. Effects of Ti6Al4V Surfaces Manufactured through Precision Centrifugal Casting and Modified by Calcium and Phosphorus Ion Implantation on Human Osteoblasts. *Metals*. 2020;10(12):1681.

doi: 10.3390/met10121681

140. Wei G, Tan M, Attarilar S, *et al*. An overview of surface modification, A way toward fabrication of nascent biomedical Ti–6Al–4V alloys. *J Mater Res Technol*. 2023;24:5896-5921.

doi: 10.1016/j.jmrt.2023.04.046

141. Bose S, Robertson SF, Bandyopadhyay A. Surface modification of biomaterials and biomedical devices using additive manufacturing. *Acta Biomater*. 2018;66:6-22.

doi: 10.1016/j.actbio.2017.11.003

142. Ebrahimi M, Kermanpur A, Kharaziha M, Bagherifard S. Engineering of multilayered coating on additively manufactured Ti-6Al-4V porous implants to promote tribological and fatigue performances. *Surf Coat Technol*. 2024;494:131400.

doi: 10.1016/j.surfcoat.2024.131400

143. Diez-Escudero A, Carlsson E, Andersson B, Järhult JD, Hailer NP. Trabecular Titanium for Orthopedic Applications: Balancing Antimicrobial with Osteoconductive Properties by Varying Silver Contents. *ACS Appl Mater Interfaces*. 2022;14(37):41751-41763.

doi: 10.1021/acsami.2c11139

144. Li L, Bai W, Wang X, Gu C, Jin G, Tu J. Mechanical Properties and in Vitro and in Vivo Biocompatibility of a-C/a-C:Ti Nanomultilayer Films on Ti6Al4V Alloy as Medical Implants. *ACS Appl Mater Interfaces*. 2017;9(19):15933-15942.

doi: 10.1021/acsami.7b02552

145. Li Y, Lu Y, Liu C. Engineered manganese phosphate coatings on titanium implants: synergistic photothermal antibiosis and ion-stimulated osteogenesis via zinc/calcium co-doping. *Rare Met*. 2025;44:10491-10513.

doi: 10.1007/s12598-025-03639-7

146. Yu D, Tang Z, Bao S, *et al*. Immunoregulatory Neuro-Vascularized Osseointegration Driven by Different Nano-Morphological CaTiO3 Bioactive Coatings on Porous Titanium Alloy Scaffolds. *Adv Healthc Mater*. 2025;14(9):2404647.

doi: 10.1002/adhm.202404647

147. Bao S, Yu D, Tang Z, *et al*. Conformationally regulated "nanozyme-like" cerium oxide with multiple free radical scavenging activities for osteoimmunology modulation and vascularized osseointegration. *Bioact Mater*. 2024;34:64-79.

doi: 10.1016/j.bioactmat.2023.12.006

148. Wu SC, Hsu HC, Wu WH, Ho WF. Enhancing Bioactivity and Mechanical Properties of Nano-Hydroxyapatite Derived from Oyster Shells through Hydrothermal Synthesis. *Nanomaterials*. 2024;14(15):1281.

doi: 10.3390/nano14151281

149. Yu X, Xu R, Zhang Z, *et al*. Different Cell and Tissue Behavior of Micro-/Nano-Tubes and Micro-/Nano-Nets Topographies on Selective Laser Melting Titanium to Enhance Osseointegration. *Int J Nanomedicine*. 2021;16:3329-3342.

doi: 10.2147/IJN.S303770

150. Rajendran A, Kapoor U, Jothinarayanan N, Lenka N, Pattanayak DK. Effect of Silver-Containing Titania Layers for Bioactivity, Antibacterial Activity, and Osteogenic Differentiation of Human Mesenchymal Stem Cells on Ti Metal. *ACS Appl Bio Mater*. 2019;2(9):3808-3819.

doi: 10.1021/acsabm.9b00420

151. Luo Y, Jiang Y, Zhu J, Tu J, Jiao S. Surface treatment functionalization of sodium hydroxide onto 3D printed porous Ti6Al4V for improved biological activities and osteogenic potencies. *J Mater Res Technol*. 2020;9(6):13661-13670.

doi: 10.1016/j.jmrt.2020.09.076

152. Wu C, Ramaswamy Y, Gale D, *et al*. Novel sphene coatings on Ti–6Al–4V for orthopedic implants using sol–gel method. *Acta Biomater*. 2008;4(3):569-576.

doi: 10.1016/j.actbio.2007.11.005

153. Yetim T, Tekdir H, Taftalı M, Turalıoğlu K, Yetim AF. Synthesis and characterisation of single and duplex ZnO/TiO2 ceramic films on additively manufactured bimetallic material of 316L stainless steel and Ti6Al4V. *Surf Topogr Metrol Prop*. 2023;11(2):024005.

doi: 10.1088/2051-672X/accf6c

154. Dong H, Li T, Tang Z, *et al*. Dual-Functional 3D-Printed Porous Titanium–Hydrogel Composite Scaffold With Mg2+ and ZIF-8 Release for Enhanced Bone Regeneration and Bacterial Inhibition. *Small Struct*. 2026;7(3):e202500861.

doi: 10.1002/sstr.202500861

155. Ma Z, Zhao Y, Xu Z, *et al*. 3D-printed porous titanium rods equipped with vancomycin-loaded hydrogels and polycaprolactone membranes for intelligent antibacterial drug release. *Sci Rep*. 2024;14(1):21749.

doi: 10.1038/s41598-024-72457-1

156. He S, Zhu J, Jing Y, *et al*. Effect of 3D-Printed Porous Titanium Alloy Pore Structure on Bone Regeneration: A Review. *Coatings*. 2024;14(3):253.

doi: 10.3390/coatings14030253

157. Wang B, Luo M, Shi Z, *et al*. Porous titanium alloys for medical application: Progress in preparation process and surface modification research. *Mater Sci Addit Manuf*. 2024;3(1):2753.

doi: 10.36922/msam.2753

158. Oh JS, Jang JH, Lee EJ. Electrophoretic Deposition of a Hybrid Graphene Oxide/Biomolecule Coating Facilitating Controllable Drug Loading and Release. *Metals*. 2021;11(6):899.

doi: 10.3390/met11060899

159. Fan D, Ding K, Lu J, Zhao Z, Mao Y, Yang G. Application of electrochemical deposition of CeO2 nanoparticles modified 3D printed porous Ti6Al4V scaffold in bone defect repair. *Biomed Mater*. 2025;20(1):015031.

doi: 10.1088/1748-605X/ada23e

160. Wei X, Chen Q, Bu L, *et al*. Improved Muscle Regeneration into a Joint Prosthesis with Mechano-Growth Factor Loaded within Mesoporous Silica Combined with Carbon Nanotubes on a Porous Titanium Alloy. *ACS Nano*. 2022;16(9):14344-14361.

doi: 10.1021/acsnano.2c04591

161. Campoccia D, Montanaro L, Arciola CR. A review of the biomaterials technologies for infection-resistant surfaces. *Biomaterials*. 2013;34(34):8533-8554.

doi: 10.1016/j.biomaterials.2013.07.089

162. Gunputh UF, Le H, Lawton K, Besinis A, Tredwin C, Handy RD. Antibacterial properties of silver nanoparticles grown in situ and anchored to titanium dioxide nanotubes on titanium implant against Staphylococcus aureus. *Nanotoxicology*. 2020;14(1):97-110.

doi: 10.1080/17435390.2019.1665727

163. Yang Y, Liu L, Luo H, Zhang D, Lei S, Zhou K. Dual-Purpose Magnesium-Incorporated Titanium Nanotubes for Combating Bacterial Infection and Ameliorating Osteolysis to Realize Better Osseointegration. *ACS Biomater Sci Eng*. 2019;5(10):5368-5383.

doi: 10.1021/acsbiomaterials.9b00938

164. He P, Zhang H, Li Y, *et al*. 1α,25-Dihydroxyvitamin D3-loaded hierarchical titanium scaffold enhanced early osseointegration. *Mater Sci Eng C*. 2020;109:110551.

doi: 10.1016/j.msec.2019.110551

165. Yang X, Wang FH, Wang WL, Liu SF, Chen YQ, Tang HP. Comparison of two-step surface treatment on surface roughness and corrosion resistance of TC4 alloy parts prepared by SLM and SEBM. *J Alloys Compd*. 2022;921:165929.

doi: 10.1016/j.jallcom.2022.165929

166. Liu L, Ma F, Kang B, *et al*. Preparation and mechanical and biological performance of the Sr-containing microarc oxidation layer on titanium implants. *Surf Coat Technol*. 2023;463:129530.

doi: 10.1016/j.surfcoat.2023.129530

167. Kołodziejska B, Stępień N, Kolmas J. The Influence of Strontium on Bone Tissue Metabolism and Its Application in Osteoporosis Treatment. *Int J Mol Sci*. 2021;22(12):6564.

doi: 10.3390/ijms22126564

168. Li Q, Yang W, Liu C, Wang D, Liang J. Correlations between the growth mechanism and properties of micro-arc oxidation coatings on titanium alloy: Effects of electrolytes. *Surf Coat Technol*. 2017;316:162-170.

doi: 10.1016/j.surfcoat.2017.03.021

169. Zhang Y, Xiu P, Jia Z, *et al*. Effect of vanadium released from micro-arc oxidized porous Ti6Al4V on biocompatibility in orthopedic applications. *Colloids Surf B Biointerfaces*. 2018;169:366-374.

doi: 10.1016/j.colsurfb.2018.05.044

170. Liu W, Li W, Wang H, Bian H, Zhang K. Surface Modification of Porous Titanium and Titanium Alloy Implants Manufactured by Selective Laser Melting: A Review. *Adv Eng Mater*. 2023;25(21):2300765.

doi: 10.1002/adem.202300765

171. Chen Z, Wang B, Yang C, *et al*. 3D Printed Pedicle Screws with Microarc Oxidation Ceramic Interfaces Enhance Osteointegration and Orthopedic Fixation Feasibility. *ACS Appl Mater Interfaces*. 2024;16(25):31983-31996.

doi: 10.1021/acsami.4c03628

172. Yang X, Wu L, Li C, *et al*. Synergistic Amelioration of

Osseointegration and Osteoimmunomodulation with a Microarc Oxidation-Treated Three-Dimensionally Printed Ti-24Nb-4Zr-8Sn Scaffold via Surface Activity and Low Elastic Modulus. *ACS Appl Mater Interfaces*. 2024;16(3):3171-3186.

doi: 10.1021/acsami.3c16459

173. Zhao P, Liu H, Deng H, *et al*. A study of chitosan hydrogel with embedded mesoporous silica nanoparticles loaded by ibuprofen as a dual stimuli-responsive drug release system for surface coating of titanium implants. *Colloids Surf B Biointerfaces*. 2014;123:657-663.

doi: 10.1016/j.colsurfb.2014.10.013

174. Fischer NG, Chen X, Astleford-Hopper K, *et al*. Antimicrobial and enzyme-responsive multi-peptide surfaces for bone-anchored devices. *Mater Sci Eng C*. 2021;125:112108.

doi: 10.1016/j.msec.2021.112108

175. Nie R, Sun Y, Lv H, *et al*. 3D printing of MXene composite hydrogel scaffolds for photothermal antibacterial activity and bone regeneration in infected bone defect models. *Nanoscale*. 2022;14(22):8112-8129.

doi: 10.1039/D2NR02176E

176. Ji Z, Wan Y, Zou Y, Wang H, Liang X, Liu P. Dual-release 3D-printed porous Ti–6Al–4V implant with drug-eluting photothermal micro-nanotopographies: combating osteosarcoma recurrence, infections, and enhancing osteogenesis. *Biomaterials*. 2026;327:123749.

doi: 10.1016/j.biomaterials.2025.123749

177. Chen Z, Cao Z, Li Z, Liu G, Zhou F, Liu W. Photothermal Lubricating Composite Hydrogel Coating with Hydrated Polymer Brushes and Load-Bearing Micropores on Ti6Al4V Implants. *Small*. 2026;22(4):e12945.

doi: 10.1002/smll.202512945

178. Wang C, Wang Y, Li X, *et al*. 3D-printed titanium scaffolds coated with a multifunctional photothermal-responsive hydrogel promote osteoporotic bone defect repair. *Mater Today Bio*. 2026;37:102879.

doi: 10.1016/j.mtbio.2026.102879

179. Chen C, Wang M, Yue X, *et al*. Ultrasound-responsive drug-carrying microbubbles combined with piezoelectric porous titanium scaffolds for the treatment of infected bone defects. *Mater Today Bio*. 2025;35:102389.

doi: 10.1016/j.mtbio.2025.102389

180. Luo L, Zheng W, Li J, *et al*. 3D-Printed Titanium Trabecular Scaffolds with Sustained Release of Hypoxia-Induced Exosomes for Dual-Mimetic Bone Regeneration. *Adv Sci*. 2025;12(23):2500599.

doi: 10.1002/advs.202500599

181. Che Z, Sheng X, Wu Y, *et al*. Sequential release of bioactive factors from functionalized metal-organic framework hydrogel enhances interfacial osseointegration of 3D-printed titanium alloy porous scaffolds. *Theranostics*. 2026;16(2):852-875.

doi: 10.7150/thno.120711

182. Palmquist A, Jolic M, Hryha E, Shah FA. Complex geometry and integrated macro-porosity: Clinical applications of electron beam melting to fabricate bespoke bone-anchored implants. *Acta Biomater*. 2023;156:125-145.

doi: 10.1016/j.actbio.2022.06.002

183. Beltrán V, Weber B, Lillo R, *et al*. Histomorphometric Analysis of Osseointegrated Grade V Titanium Mini Transitional Implants in Edentulous Mandible by Backscattered Scanning Electron Microscopy (BS-SEM). *Metals*. 2020;11(1):2.

doi: 10.3390/met11010002

184. Gupta K, Meena K. Artificial bone scaffolds and bone joints by additive manufacturing: A review. *Bioprinting*. 2023;31:e00268.

doi: 10.1016/j.bprint.2023.e00268

185. Guo L, Ataollah Naghavi S, Wang Z, *et al*. On the design evolution of hip implants: A review. *Mater Des*. 2022;216:110552.

doi: 10.1016/j.matdes.2022.110552

186. Xu L, Qin H, Tan J, *et al*. Clinical study of 3D printed personalized prosthesis in the treatment of bone defect after pelvic tumor resection. *J Orthop Transl*. 2021;29:163-169.

doi: 10.1016/j.jot.2021.05.007

187. Siu TL, Rogers JM, Lin K, Thompson R, Owbridge M. Custom-Made Titanium 3-Dimensional Printed Interbody Cages for Treatment of Osteoporotic Fracture–Related Spinal Deformity. *World Neurosurg*. 2018;111:1-5.

doi: 10.1016/j.wneu.2017.11.160

188. Cheng J, Gao Y, Long Z, Pei G, Li Z, Meng G. Repair of distal fibular and lateral malleolus defects with individualized 3D-printed titanium alloy prosthesis: The first case report from China. *Int J Surg Case Rep*. 2022;94:107057.

doi: 10.1016/j.ijscr.2022.107057

189. Sharma M, Soni M. Direct metal laser sintering of TI6Al4V alloy for patient-specific temporo mandibular joint prosthesis and implant. *Mater Today Proc*. 2021;38:333-339.

doi: 10.1016/j.matpr.2020.07.417

190. Bregoli C, Stacchiotti F, Fiocchi J, *et al*. A biomechanical study of osseointegrated patient-matched additively manufactured implant for treatment of thumb amputees. *Med Eng Phys*. 2023;118:104019.

doi: 10.1016/j.medengphy.2023.104019

191. Zhang LC, Klemm D, Eckert J, Hao YL, Sercombe TB. Manufacture by selective laser melting and mechanical behavior of a biomedical Ti–24Nb–4Zr–8Sn alloy. *Scr*

Mater. 2011;65(1):21-24.

doi: 10.1016/j.scriptamat.2011.03.024

192. Li L, Shi J, Zhang K, *et al*. Early osteointegration evaluation of porous Ti6Al4V scaffolds designed based on triply periodic minimal surface models. *J Orthop Transl*. 2019;19:94-105.

doi: 10.1016/j.jot.2019.03.003

193. Rana M, Karmakar S, Bandyopadhyay A, Roychowdhury A. Design and manufacturing of patient-specific Ti6Al4V implants with inhomogeneous porosity. *J Mech Behav Biomed Mater*. 2023;143:105925.

doi: 10.1016/j.jmbbm.2023.105925

194. Chowdhury S, Arunachalam N. Surface functionalization of additively manufactured titanium alloy for orthopaedic implant applications. *J Manuf Process*. 2023;102:387-405.

doi: 10.1016/j.jmapro.2023.07.015

195. Li Y, Wang F. Review of 3D-Printed Titanium-Based Implants: Materials and Post-Processing. *ChemBioEng Rev*. 2024;11(6):e202400032.

doi: 10.1002/cben.202400032

196. Chen A, Li K, Li Y, *et al*. Occlusion-activated autonomous piezoelectric implants for adaptive prevention of peri-implantitis. *Nat Commun*. 2026.

doi: 10.1038/s41467-026-71556-z

197. Xiong Y, Wang W, Gao R, *et al*. Fatigue behavior and osseointegration of porous Ti-6Al-4V scaffolds with dense core for dental application. *Mater Des*. 2020;195:108994.

doi: 10.1016/j.matdes.2020.108994

198. Iezzi G, Zavan B, Petrini M, *et al*. 3D printed dental implants with a porous structure: The in vitro response of osteoblasts, fibroblasts, mesenchymal stem cells, and monocytes. *J Dent*. 2024;140:104778.

doi: 10.1016/j.jdent.2023.104778

199. Tunchel S, Blay A, Kolerman R, Mijiritsky E, Shibli JA. 3D Printing/Additive Manufacturing Single Titanium Dental Implants: A Prospective Multicenter Study with 3 Years of Follow-Up. *Int J Dent*. 2016;2016:1-9.

doi: 10.1155/2016/8590971